ResearchGate

See discussions, stats, and author profiles for this publication at: https://www.researchgate.net/publication/23169134

FIR Filter Banks for Hexagonal Data Processing

Article *in* IEEE Transactions on Image Processing · October 2008

DOI: 10.1109/TIP.2008.2001401 · Source: PubMed

CITATIONS
10

READS
27

1 author:

Qingtang Jiang
University of Missouri - St. Louis
84 PUBLICATIONS **1,406** CITATIONS

SEE PROFILE

Some of the authors of this publication are also working on these related projects:

Computer aided design View project

All content following this page was uploaded by Qingtang Jiang on 24 February 2015.

The user has requested enhancement of the downloaded file.

FIR Filter Banks for Hexagonal Data Processing

Qingtang Jiang

***Abstract*—Images are conventionally sampled on a rectangular lattice, and they are also commonly stored as such a lattice. Thus, traditional image processing is carried out on the rectangular lattice. The hexagonal lattice was proposed more than four decades ago as an alternative method for sampling. Compared with the rectangular lattice, the hexagonal lattice has certain advantages which include that it needs less sampling points; it has better consistent connectivity and higher symmetry; and that the hexagonal structure is pertinent to the vision process. In this paper we investigate the construction of symmetric FIR hexagonal filter banks for multiresolution hexagonal image processing. We obtain block structures of FIR hexagonal filter banks with 3-fold rotational symmetry and 3-fold axial symmetry. These block structures yield families of orthogonal and biorthogonal FIR hexagonal filter banks with 3-fold rotational symmetry and 3-fold axial symmetry. In this paper, we also discuss the construction of orthogonal and biorthogonal FIR filter banks with scaling functions and wavelets having optimal smoothness. In addition, we present some of such orthogonal and biorthogonal FIR filters banks.**

***Index Terms*—Hexagonal lattice, hexagonal data, 3-fold rotational symmetry, 3-fold axial symmetry, orthogonal FIR hexagonal filter bank, biorthogonal FIR hexagonal filter bank, compactly supported orthogonal and biorthogonal hexagonal wavelets.**

EDICS Category: MRP-FBNK

I. Introduction

Traditional 2-D data (image) processing is carried out on the rectangular lattice since 2-D data is conventionally sampled at the sites (points) on a square or rectangular lattice and it is also commonly stored as such a lattice. See a square lattice in the left part of Fig. 1. The hexagonal lattice (in the right part of Fig. 1) was proposed more than four decades ago as an alternative method for sampling. Compared with a rectangular lattice, a hexagonal lattice has certain advantages [1]-[9]. It was shown in [1] that, for functions band-limited in a circular region in the frequency domain, the hexagonal lattice needs a smaller number (about 13.4% smaller) of sampling points to maintain equally high frequency information than the square lattice. The hexagonal structure has better consistent connectivity: each elementary cell of a hexagonal lattice has six neighbors of the same type while an elementary cell of a square lattice has two different types of neighbors. The hexagonal structure possesses higher symmetry: a regular hexagonal lattice has 12-fold symmetry while a square lattice has 8-fold symmetry. Other advantages of the hexagonal structure over the square structure include that it offers greater angular resolution of images and it is closely related to the human visual system. Hence, the hexagonal lattice has been used in many areas such as edge detection [10], [11] and pattern recognition [12]-[16]. The hexagonal lattice has also been applied in Geoscience and other fields. For example, in the Soil Moisture and Ocean Salinity (SMOS) space mission led by the European Space Agency, the data collected by the Y-shaped antenna of the SMOS space mission is hexagonal data (sampled on a hexagonal lattice) [17], [18]. A hexagon-based grid has been adopted by the U.S. Environmental Protection Agency for global sampling problems [19], [20].

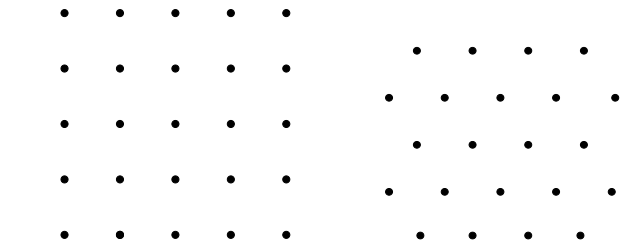

Fig. 1. *Rectangular lattice (left) and hexagonal lattice (right)*

Research on hexagonal image processing goes back to Petersen and Middleton [1] over 40 years ago. Since then, researchers in different areas have made many contributions in the study of hexagonal image processing on various topics, see [7]-[9] and the references therein. Multiscale (multiresolution) image processing has been one of the most popular areas of research investigation in various scientific and engineering disciplines during the decade of the 1990's, and it has been used in many applications. However, as it was pointed out in [7], multiresolution hexagonal image processing is a research area with a slow pace of activity. One probable reason for this could be that most researchers in the "Wavelets" community are accustomed to the traditional rectangular lattice. Another reason is probably that current approaches have encountered difficulties in the construction and design of desirable hexagonal filter banks to be used for multiresolution image processing. To the author's best knowledge, [21]-[25], [4], [26] are the papers available on the construction/design of hexagonal filter banks with both lowpass and highpass filters constructed. [21] presented a few FIR (finite impulse response) hexagonal filter banks which achieved near orthogonality. [22] provided one 7-channel ($\sqrt{7}$-refinement) FIR hexagonal filter bank for image coding. The authors in [23] designed FIR hexagonal filter banks by minimizing the filter bank error and intra-band aliasing error function and applied their filters to image compression and orientation analysis. The highpass filters used in [23] are suitable spatial shifting and frequency modulations of the lowpass filter. FIR hexagonal filter banks was also designed in [24] by the same method as in [23] but with a different filter bank error and intra-band aliasing

Q. Jiang is with the Department of Mathematics and Computer Science, University of Missouri–St. Louis, St. Louis, MO 63121, USA, e-mail: jiangq@umsl.edu , web: http://www.cs.umsl.edu/∼jiang .

Research supported by UM Research Board 10/05 and UMSL Research Award 10/06.

error function. The FIR filter banks designed in [21], [23], [24] are not perfect reconstruction filter banks. Construction of biorthogonal hexagonal filter banks was fully investigated in [25] and a few biorthogonal FIR filter banks were constructed there. However, it is difficult to construct biorthogonal filter banks with smooth wavelets by their approach which also results in filters with large filter lengths. The author in [4] (also in [26]) proposed a novel block structure of orthogonal/biorthogonal FIR hexagonal filter banks with certain symmetry. However, a rigorously mathematical proof of the symmetry and the (bi)orthogonality of the filter banks in [4] is desired, and the issue of how to select the free parameters in these filter banks needs to be addressed.

Though the hexagonal filter banks designed in [23] are not perfect reconstruction filter banks, experimental results on their applications to image compression and orientation analysis carried out in [23] and their applications to digital mammographic feature enhancement and the recognition of complex annotations in [12], [13] are appealing. Therefore, the construction/design of hexagonal filter banks deserves further investigation. The main objective of this paper is to construct orthogonal and biorthogonal FIR hexagonal filter banks with certain symmetry which is pertinent to the symmetry structure of the hexagonal lattice.

This paper is organized as follows. In Section II, we first briefly show that the problem of filter construction along the hexagonal lattice can be transformed into that along the square lattice of $\mathbf{Z}^2$. After that we discuss the symmetry of filter banks and review some basic results on orthogonal/biorthogonal filter banks. In Section III, we present block structures of orthogonal and biorthogonal FIR filter banks with 3-fold rotational symmetry. In Section IV, we provide block structures of orthogonal and biorthogonal FIR filter banks with 3-fold axial symmetry. These structures include that in [4]. In both Sections III and IV, we also discuss the construction of orthogonal and biorthogonal FIR filter banks with scaling functions and wavelets having optimal smoothness.

In this paper we use the following notations. For $\mathbf{x} = [x_1, x_2]^T, \mathbf{y} = [y_1, y_2]^T$, $\mathbf{x}\cdot\mathbf{y}$ denotes their dot (inner) product $\mathbf{x}^T\mathbf{y}$. For a function f on $\mathbb{R}^2$, $\hat{f}$ denotes its Fourier transform: $\hat{f}(\omega) = \int_{\mathbb{R}^2} f(\mathbf{x})e^{-i\mathbf{x}\cdot\omega}d\mathbf{x}$. For a matrix M, we use M^* to denote its conjugate transpose $\overline{M^T}$, and for a nonsingular matrix M, M^{-T} denotes $(M^{-1})^T$. For $\omega = [\omega_1, \omega_2]^T$, let

$$z_1 = e^{-i\omega_1},\ z_2 = e^{-i\omega_2}. \tag{1}$$

II. Preliminaries

In this section, after showing that the problem of filter construction along the hexagonal lattice can be transformed into that along the square lattice, we provide some basic results on the symmetry and the orthogonality/biorthogonality of filter banks.

A. Transforming the hexagonal lattice to the square lattice $\mathbf{Z}^2$

Most multiscale analysis theory and algorithms for image processing are developed along the square lattice with sites $\mathbf{k} \in \mathbf{Z}^2$, though they could be established along general lattices

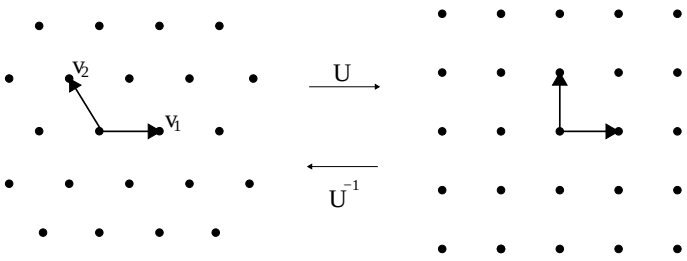

Fig. 2. *Regular unit hexagonal lattice (left) and square lattice* $\mathbf{Z}^2$ *(right)*

(see e.g. [27] for the shift-invariant theory along general lattices). To design hexagonal filter banks, here we transform the hexagonal lattice to the square lattice so that we can use the well-developed integer-shift multiscale analysis theory and methods.

Let $\mathcal{G}$ be the regular unit hexagonal lattice defined by

$$\mathcal{G} = \{n_1\mathbf{v}_1 + n_2\mathbf{v}_2 : \quad n_1, n_2 \in \mathbf{Z}\}, \tag{2}$$

where

$$\mathbf{v}_1 = [1, 0]^T, \quad \mathbf{v}_2 = [-\frac{1}{2}, \frac{\sqrt{3}}{2}]^T.$$

Let U be the matrix defined by

$$U = \begin{bmatrix} 1 & \frac{\sqrt{3}}{3} \\ 0 & \frac{2\sqrt{3}}{3} \end{bmatrix}. \tag{3}$$

Then U transforms the regular unit hexagonal lattice into the square lattice with sites $\mathbf{k}$, $\mathbf{k} \in \mathbf{Z}^2$. See Fig. 2.

For a hexagonal filter $H(\omega) = \frac{1}{4}\sum_{\mathbf{g}\in\mathcal{G}} H_{\mathbf{g}}e^{-i\mathbf{g}\cdot\omega}$ with its (real) impulse response $H_{\mathbf{g}}$ (in this paper a factor $\frac{1}{4}$ is added for the convenience), by the transformation with the matrix U, we have a corresponding filter $h(\omega) = \frac{1}{4}\sum_{\mathbf{k}\in\mathbf{Z}^2} h_{\mathbf{k}}e^{-i\mathbf{k}\cdot\omega}$ for square data (squarely sampled data) with its impulse response $h_{\mathbf{k}} = H_{U^{-1}\mathbf{k}}$. Conversely, corresponding to a square filter (filter for square data) $h(\omega) = \frac{1}{4}\sum_{\mathbf{k}\in\mathbf{Z}^2} h_{\mathbf{k}}e^{-i\mathbf{k}\cdot\omega}$, we have a hexagonal filter $H(\omega) = \frac{1}{4}\sum_{\mathbf{g}\in\mathcal{G}} h_{U\mathbf{g}}e^{-i\mathbf{g}\cdot\omega}$. In the frequency domain, the relationship between $H(\omega)$ and $h(\omega)$ (with $h_{\mathbf{k}} = H_{U^{-1}\mathbf{k}}$) are given by

$$H(\omega) = h(U^{-T}\omega).$$

The matrix U also transforms the scaling functions and wavelets along the hexagonal lattice to those along the square lattice $\mathbf{Z}^2$. For example, if Φ is the scaling function associated with a lowpass hexagonal filter $H(\omega) = \frac{1}{4}\sum_{\mathbf{g}\in\mathcal{G}} H_{\mathbf{g}}e^{-i\mathbf{g}\cdot\omega}$, namely, it satisfies

$$\Phi(\mathbf{x}) = \sum_{\mathbf{g}\in\mathcal{G}} H_{\mathbf{g}}\Phi(2\mathbf{x} - \mathbf{g}), \quad \mathbf{x} \in \mathbb{R}^2,$$

then ϕ defined by

$$\phi(\mathbf{x}) = \Phi(U^{-1}\mathbf{x})$$

is the scaling function associated with square filter $h(\omega) = \frac{1}{4}\sum_{\mathbf{k}\in\mathbf{Z}^2} h_{\mathbf{k}}e^{-i\mathbf{k}\cdot\omega}$, where $h_{\mathbf{k}} = H_{U^{-1}\mathbf{k}}$. Therefore, to design hexagonal filters, we need only to construct filters along the traditional lattice $\mathbf{Z}^2$. Then the matrix U will transform the filters, scaling functions and wavelets along the lattice $\mathbf{Z}^2$ into those along the hexagonal lattice.

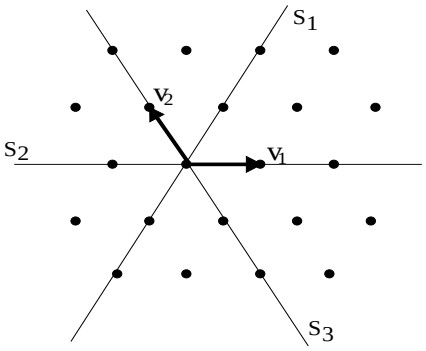

Fig. 3. *Lines S_1, S_2, S_3 in hexagonal lattice*

B. Symmetry of filter banks

Since the hexagonal lattice has the highest degree of symmetry, it is desirable that hexagonal filter banks designed also have certain symmetry pertinent to the symmetric structure of the hexagonal lattice. In this paper, we consider two types of symmetry: 3-fold rotational symmetry and 3-fold axial symmetry which are defined below.

Definition 1: A hexagonal filter bank $\{P, Q^{(1)}, Q^{(2)}, Q^{(3)}\}$ is said to have 3-*fold rotational symmetry* if its lowpass filter $P(\omega)$ is invariant under the $\frac{2}{3}\pi$ and $\frac{4}{3}\pi$ rotations, and its highpass filters $Q^{(2)}$ and $Q^{(3)}$ are the $\frac{2}{3}\pi$ and $\frac{4}{3}\pi$ (anticlockwise) rotations of highpass filter $Q^{(1)}$, respectively.

Let S_1, S_2 and S_3 be the lines in the regular unit hexagonal lattice shown in Fig. 3. Namely, S_1, S_2 and S_3 are the lines passing through the origin with slopes $\sqrt{3}$, 0 and $-\sqrt{3}$, respectively.

Definition 2: A hexagonal filter bank $\{P, Q^{(1)}, Q^{(2)}, Q^{(3)}\}$ is said to have 3-*fold axial symmetry* (or 3-fold line symmetry) if its lowpass filter $P(\omega)$ is symmetric around S_1, S_2 and S_3, and its highpass filter $Q^{(1)}$ is symmetric around the axis S_1 and other two highpass filters $Q^{(2)}$ and $Q^{(3)}$ are the $\frac{2}{3}\pi$ and $\frac{4}{3}\pi$ (anticlockwise) rotations of $Q^{(1)}$, respectively.

Let $\widetilde{R}_1, \widetilde{R}_2, \widetilde{N}_e, \widetilde{W}$ and $\widetilde{S}_e$ be the matrices defined by

$$\widetilde{R}_1 = \begin{bmatrix} -\frac{1}{2} & \frac{\sqrt{3}}{2} \\ -\frac{\sqrt{3}}{2} & -\frac{1}{2} \end{bmatrix}, \ \widetilde{R}_2 = \begin{bmatrix} -\frac{1}{2} & -\frac{\sqrt{3}}{2} \\ \frac{\sqrt{3}}{2} & -\frac{1}{2} \end{bmatrix},$$
$$\widetilde{N}_e = \begin{bmatrix} -\frac{1}{2} & \frac{\sqrt{3}}{2} \\ \frac{\sqrt{3}}{2} & \frac{1}{2} \end{bmatrix}, \ \widetilde{W} = \begin{bmatrix} 1 & 0 \\ 0 & -1 \end{bmatrix},$$
$$\widetilde{S}_e = \begin{bmatrix} -\frac{1}{2} & -\frac{\sqrt{3}}{2} \\ -\frac{\sqrt{3}}{2} & \frac{1}{2} \end{bmatrix}.$$

Then one can easily show that $\{P, Q^{(1)}, Q^{(2)}, Q^{(3)}\}$ has 3-fold rotational symmetry if and only if for all $\mathbf{g} \in \mathcal{G}$,

$$P_{\widetilde{R}_1\mathbf{g}} = P_{\widetilde{R}_2\mathbf{g}} = P_{\mathbf{g}}, \ Q^{(2)}_{\mathbf{g}} = Q^{(1)}_{\widetilde{R}_1\mathbf{g}}, \ Q^{(3)}_{\mathbf{g}} = Q^{(1)}_{\widetilde{R}_2\mathbf{g}}; \quad (4)$$

and that $\{P, Q^{(1)}, Q^{(2)}, Q^{(3)}\}$ has 3-fold axial symmetry if and only if for all $\mathbf{g} \in \mathcal{G}$,

$$\begin{cases} P_{\widetilde{N}_e\mathbf{g}} = P_{\widetilde{W}\mathbf{g}} = P_{\widetilde{S}_e\mathbf{g}} = P_{\mathbf{g}}, \\ Q^{(1)}_{\widetilde{N}_e\mathbf{g}} = Q^{(1)}_{\mathbf{g}}, \ Q^{(2)}_{\mathbf{g}} = Q^{(1)}_{\widetilde{R}_1\mathbf{g}}, \ Q^{(3)}_{\mathbf{g}} = Q^{(1)}_{\widetilde{R}_2\mathbf{g}}. \end{cases} \quad (5)$$

Observe that $\widetilde{R}_1 = \widetilde{W}\widetilde{N}_e$, $\widetilde{R}_2 = \widetilde{S}_e\widetilde{N}_e$. Thus if $\{P, Q^{(1)}, Q^{(2)}, Q^{(3)}\}$ satisfies (5), then it satisfies (4). Therefore, if a hexagonal filter bank has 3-fold axial symmetry, then it has 3-fold rotational symmetry.

The 3-fold rotational symmetry is considered in [25], where it is called the hexagonal symmetry. Both the 3-fold rotational symmetry and the 3-fold axial symmetry are closely related to the symmetry structure of the hexagonal lattice. In this paper we consider filter banks with these two types of symmetry. Compared with filter banks with 3-fold axial symmetry, filter banks with 3-fold rotational symmetry have less symmetry but they provide more flexibility for the construction of filters. It should be up to one's specific application to choose filter banks with 3-fold rotational or axial symmetry.

For a hexagonal filter bank $\{P, Q^{(1)}, Q^{(2)}, Q^{(3)}\}$, let $\{p, q^{(1)}, q^{(2)}, q^{(3)}\}$ be the corresponding square filter bank after the transformation by the matrix U in (3). Namely, the impulse responses $p_{\mathbf{k}}, q^{(\ell)}_{\mathbf{k}}$ of $p(\omega), q^{(\ell)}(\omega), 1 \le \ell \le 3$ are $P_{U^{-1}\mathbf{k}}, Q^{(\ell)}_{U^{-1}\mathbf{k}}$, respectively. Let R_1, R_2, N_e, W and S_e denote the matrices $U\widetilde{R}_1U^{-1}$, $U\widetilde{R}_2U^{-1}$, $U\widetilde{N}_eU^{-1}$, $U\widetilde{W}U^{-1}$ and $U\widetilde{S}_eU^{-1}$ respectively, namely,

$$R_1 = \begin{bmatrix} -1 & 1 \\ -1 & 0 \end{bmatrix}, R_2 = \begin{bmatrix} 0 & -1 \\ 1 & -1 \end{bmatrix}, \quad (6)$$

$$N_e = \begin{bmatrix} 0 & 1 \\ 1 & 0 \end{bmatrix}, W = \begin{bmatrix} 1 & -1 \\ 0 & -1 \end{bmatrix}, S_e = \begin{bmatrix} -1 & 0 \\ -1 & 1 \end{bmatrix}. \quad (7)$$

Then one can show that $P, Q^{(1)}, Q^{(2)}, Q^{(3)}$ satisfy (4) if and only if

$$p_{R_1\mathbf{k}} = p_{R_2\mathbf{k}} = p_{\mathbf{k}}, \ q^{(2)}_{\mathbf{k}} = q^{(1)}_{R_1\mathbf{k}}, \ q^{(3)}_{\mathbf{k}} = q^{(1)}_{R_2\mathbf{k}}, \ \mathbf{k} \in \mathbf{Z}^2; \quad (8)$$

and that $P, Q^{(1)}, Q^{(2)}, Q^{(3)}$ satisfy (5) if and only if

$$\begin{cases} p_{N_e\mathbf{k}} = p_{W\mathbf{k}} = p_{S_e\mathbf{k}} = p_{\mathbf{k}}, \\ q^{(1)}_{N_e\mathbf{k}} = q^{(1)}_{\mathbf{k}}, \ q^{(2)}_{\mathbf{k}} = q^{(1)}_{R_1\mathbf{k}}, \ q^{(3)}_{\mathbf{k}} = q^{(1)}_{R_2\mathbf{k}}, \ \mathbf{k} \in \mathbf{Z}^2. \end{cases} \quad (9)$$

To summarize, we have the following proposition.

Proposition 1: Let $\{P, Q^{(1)}, Q^{(2)}, Q^{(3)}\}$ be a hexagonal filter bank and $\{p, q^{(1)}, q^{(2)}, q^{(3)}\}$ be its corresponding square filter bank. Then $\{P, Q^{(1)}, Q^{(2)}, Q^{(3)}\}$ has 3-fold rotational symmetry if and only if $\{p, q^{(1)}, q^{(2)}, q^{(3)}\}$ satisfies (8); and $\{P, Q^{(1)}, Q^{(2)}, Q^{(3)}\}$ has 3-fold axial symmetry if and only if $\{p, q^{(1)}, q^{(2)}, q^{(3)}\}$ satisfies (9).

In the following, for the convenience, we say a square filter bank $\{p, q^{(1)}, q^{(2)}, q^{(3)}\}$ has 3-*fold rotational symmetry* (3-*fold axial symmetry* resp.) if it satisfies (8) ((9) resp.).

C. Biorthogonality, sum rule order and smoothness

In this subsection, we review some results on orthogonal/biorthogonal (square) filter banks. Denote

$$\eta_0 = [0,0]^T, \ \eta_1 = [\pi,\pi]^T, \ \eta_2 = [\pi,0]^T, \ \eta_3 = [0,\pi]^T. \quad (10)$$

FIR filter banks $\{p, q^{(1)}, q^{(2)}, q^{(3)}\}$ and $\{\tilde{p}, \tilde{q}^{(1)}, \tilde{q}^{(2)}, \tilde{q}^{(3)}\}$ are said to be *biorthogonal* or they are perfect reconstruction filter

banks if

$$\sum_{0\le k\le 3} p(\omega+\eta_k)\overline{\tilde{p}(\omega+\eta_k)} = 1, \tag{11}$$

$$\sum_{0\le k\le 3} p(\omega+\eta_k)\overline{\tilde{q}^{(\ell)}(\omega+\eta_k)} = 0, \quad 1\le \ell\le 3, \tag{12}$$

$$\sum_{0\le k\le 3} q^{(\ell')}(\omega+\eta_k)\overline{\tilde{q}^{(\ell)}(\omega+\eta_k)} = \delta_{\ell'-\ell}, \tag{13}$$

for $1\le \ell,\ell'\le 3$, $\omega\in \mathbb{R}^2$, where δ_ℓ is the kronecker-delta sequence. A filter bank $\{p, q^{(1)}, q^{(2)}, q^{(3)}\}$ is said to be *orthogonal* if it satisfies (11)-(13) with $\tilde{p}=p, \tilde{q}^{(\ell)}=q^{(\ell)}, 1\le\ell\le 3$.

Let ϕ and $\tilde{\phi}$ be the scaling function associated with p and $\tilde{p}$ respectively. Then (11) is the necessary condition for ϕ and $\tilde{\phi}$ to be biorthogonal duals:

$$\int_{\mathbb{R}^2} \phi(\mathbf{x})\overline{\tilde{\phi}(\mathbf{x}-\mathbf{k})}\,d\mathbf{x} = \delta_{k_1}\delta_{k_2}, \tag{14}$$

for all $\mathbf{k}=[k_1,k_2]^T\in\mathbf{Z}^2$. We say ϕ is orthogonal if it satisfies (14) with $\tilde{\phi}=\phi$. Under certain mild conditions, the condition (11) is also sufficient for the biorthogonality of ϕ and $\tilde{\phi}$. For example, if the cascade algorithms associated with p and $\tilde{p}$ are convergent, or under a stronger condition that both ϕ and $\tilde{\phi}$ are stable, then the biorthogonality of p and $\tilde{p}$ (orthogonality of p resp.) imply that ϕ and $\tilde{\phi}$ are biorthogonal duals (ϕ is orthogonal resp.) (see e.g. [28], [29]). One can check the convergence of the cascade algorithm associated with a given p by calculating the eigenvalues of the so-called transition operator associated with p, see e.g. [30] for the details. For biorthogonal FIR filter banks $\{p, q^{(1)}, q^{(2)}, q^{(3)}\}$ and $\{\tilde{p}, \tilde{q}^{(1)}, \tilde{q}^{(2)}, \tilde{q}^{(3)}\}$, if the associated scaling functions ϕ and $\tilde{\phi}$ are biorthogonal duals, then $\psi^{(\ell)}, \tilde{\psi}^{(\ell)}$ defined by

$$\widehat{\psi^{(\ell)}}(\omega) = q^{(\ell)}(\frac{\omega}{2})\widehat{\phi}(\frac{\omega}{2}), \quad \widehat{\tilde{\psi}^{(\ell)}}(\omega) = \tilde{q}^{(\ell)}(\frac{\omega}{2})\widehat{\tilde{\phi}}(\frac{\omega}{2}),$$

are biorthogonal wavelets, namely, $\{\psi^{(\ell)}_{j,\mathbf{k}} : 1\le\ell\le 3, j\in\mathbf{Z}, \mathbf{k}\in\mathbf{Z}^2\}$ and $\{\tilde{\psi}^{(\ell)}_{j,\mathbf{k}} : 1\le\ell\le 3, j\in\mathbf{Z}, \mathbf{k}\in\mathbf{Z}^2\}$ are biorthogonal bases of $L^2(\mathbb{R}^2)$, where

$$\psi^{(\ell)}_{j,\mathbf{k}}(\mathbf{x}) = 2^j\psi^{(\ell)}(2^j\mathbf{x}-\mathbf{k}),\ \tilde{\psi}^{(\ell)}_{j,\mathbf{k}}(\mathbf{x}) = 2^j\tilde{\psi}^{(\ell)}(2^j\mathbf{x}-\mathbf{k}).$$

Similarly, for an orthogonal filter bank $\{p, q^{(1)}, q^{(2)}, q^{(3)}\}$, if the associated scaling function ϕ is orthogonal, then $\psi^{(\ell)}$ defined above are orthogonal wavelets, namely, $\{\psi^{(\ell)}_{j,\mathbf{k}} : 1\le\ell\le 3, j\in\mathbf{Z}, \mathbf{k}\in\mathbf{Z}^2\}$ is an orthogonal basis of $L^2(\mathbb{R}^2)$. The reader is referred to [31] and [32] for the multiscale analysis theory and its applications.

For a (lowpass) filter $p(\omega)=\frac{1}{4}\sum_{\mathbf{k}\in\mathbf{Z}^2} p_{\mathbf{k}}e^{-i\mathbf{k}\cdot\omega}$, we say that $p(\omega)$ has sum rules of order m if $\sum_{\mathbf{k}} p_{\mathbf{k}}=4$, and

$$\begin{aligned}
&\sum_{\mathbf{k}}(2k_1)^{\alpha_1}(2k_2)^{\alpha_2}p_{(2k_1,2k_2)}\\
&=\sum_{\mathbf{k}}(2k_1+1)^{\alpha_1}(2k_2)^{\alpha_2}p_{(2k_1+1,2k_2)}\\
&=\sum_{\mathbf{k}}(2k_1)^{\alpha_1}(2k_2+1)^{\alpha_2}p_{(2k_1,2k_2+1)}\\
&=\sum_{\mathbf{k}}(2k_1+1)^{\alpha_1}(2k_2+1)^{\alpha_2}p_{(2k_1+1,2k_2+1)},
\end{aligned}$$

for all nonnegative integers α_1,α_2 with $0\le\alpha_1+\alpha_2<m$. Under certain mild conditions, sum rule order of $p(\omega)$ is equivalent to the approximation order and accuracy of the scaling function ϕ associated with $p(\omega)$. The reader sees [33] for the details. High sum rule order of $p(\omega)$ is also a necessary condition for the high smoothness order of ϕ under certain conditions such as the stability of ϕ. For example, for a stable ϕ, if it is in the Sobolev space $W^n(\mathbb{R}^2)$ (see the definition of the Sobolev space below), then its associated lowpass filter $p(\omega)$ must have sum rules of order at least $n+1$.

In the following two sections we obtain block structures of orthogonal/biorthogonal FIR filter banks with 3-fold rotational symmetry and with 3-fold axial symmetry. These orthogonal/biorthogonal filter banks are given by some free parameters. When a family of filter banks is available (given by free parameters), one can design the filters with desirable properties for one's specific applications. For example, one may consider to design filters with the optimum time-frequency localization (see [34] and [35] for the design of 1-D matrix-valued filters with the optimum time-frequency localization). In this paper we consider the filters based on the smoothness of the associated scaling functions ϕ. The smoothness of the associated wavelets $\psi^{(1)},\psi^{(2)},\psi^{(3)}$ is the same as ϕ since they are finite linear combinations of ϕ and its integer shifts. The smoothness of ϕ and its associated wavelets is important for some applications. For example, certain smoothness of them is required for the image reconstruction. In addition, a scaling function and its associated wavelets with poor smoothness result in poor frequency localization of them.

In the consideration of smoothness, we will compute the Sobolev smoothness of scaling functions. For $s\ge 0$, denote by $W^s(\mathbb{R}^2)$ the Sobolev space consisting of functions $f(\mathbf{x})$ on $\mathbb{R}^2$ with

$$\int_{\mathbb{R}^2}(1+|\omega|^2)^s|\hat{f}(\omega)|^2d\omega<\infty.$$

If $f\in W^s(\mathbb{R}^2)$ with $s>k+1$ for some positive integer k, then $f\in C^k(\mathbb{R}^2)$. We use the smoothness formula in [36] to compute the Sobolev smoothness order of scaling functions. See [37] for the detailed formulas for the Sobolev smoothness of scaling functions/vectors and [38] for algorithms and Matlab routines to find the Sobolev smoothness order.

For an FIR lowpass filter $p(\omega)$ given by some free parameters, the procedures to construct the scaling function ϕ with the (locally) optimal Sobolev smoothness are described as follows: (1) Solve the linear equations for the sum rule orders such that $p(\omega)$ has the desired sum rule order. The resulting $p(\omega)$ is still given by some (but less) free parameters. (2) Adjust the free parameters for the resulting $p(\omega)$ by applying the algorithms/software in [37]/[38] to achieve the optimal Sobolev smoothness for ϕ.

III. Orthogonal and biorthogonal FIR filter banks with 3-fold rotational symmetry

In this section we consider the construction of orthogonal and biorthogonal filter banks with 3-fold rotational symmetry. The 3-fold rotational symmetry of filter banks is discussed in §III. A, and block structures of orthogonal and biorthogonal

FIR filter banks with 3-fold rotational symmetry are presented in §III. B and §III. C, respectively.

A. FIR filter banks with 3-fold rotational symmetry

Suppose $p(\omega), q^{(1)}(\omega), q^{(2)}(\omega), q^{(3)}(\omega)$ are FIR filters with impulse response coefficients $p_{\mathbf{k}}, q_{\mathbf{k}}^{(1)}, q_{\mathbf{k}}^{(2)}, q_{\mathbf{k}}^{(3)}$. Then filter bank $\{p, q^{(1)}, q^{(2)}, q^{(3)}\}$ has 3-fold rotational symmetry, namely it satisfies (8), if and only if

$$\begin{cases} p(\omega) = p(R_1^{-T}\omega) = p(R_2^{-T}\omega), \\ q^{(2)}(\omega) = q^{(1)}(R_1^{-T}\omega),\ q^{(3)}(\omega) = q^{(1)}(R_2^{-T}\omega). \end{cases}$$

This, together with the facts that $R_2 = R_1^2, R_1^3 = I_2$, leads to the following proposition.

Proposition 2: A filter bank $\{p, q^{(1)}, q^{(2)}, q^{(3)}\}$ has 3-fold rotational symmetry if and only if it satisfies

$$\left[p,\ q^{(1)},\ q^{(2)},\ q^{(3)}\right]^T (R_1^{-T}\omega) = M_0 \left[p(\omega),\ q^{(1)}(\omega),\ q^{(2)}(\omega),\ q^{(3)}(\omega)\right]^T,$$

where

$$M_0 = \begin{bmatrix} 1 & 0 & 0 & 0 \\ 0 & 0 & 1 & 0 \\ 0 & 0 & 0 & 1 \\ 0 & 1 & 0 & 0 \end{bmatrix}. \tag{15}$$

Next, we consider the filter bank $\{p, q^{(1)}, q^{(2)}, q^{(3)}\}$ to be given by the product of block matrices. Assume that we can write $[p(\omega), q^{(1)}(\omega), q^{(2)}(\omega), q^{(3)}(\omega)]^T$ as $A(2\omega)[p_0(\omega), q_0^{(1)}(\omega), q_0^{(2)}(\omega), q_0^{(3)}(\omega)]^T$, where $A(\omega)$ is a 4×4 matrix with trigonometric polynomial entries, and $\{p_0, q_0^{(1)}, q_0^{(2)}, q_0^{(3)}\}$ is another FIR filter bank. If both $\{p, q^{(1)}, q^{(2)}, q^{(3)}\}$ and $\{p_0, q_0^{(1)}, q_0^{(2)}, q_0^{(3)}\}$ have 3-fold rotational symmetry, then Proposition 2 leads to that $A(\omega)$ satisfies

$$A(R_1^{-T}\omega) = M_0 A(\omega) M_0^{-1}, \tag{16}$$

where M_0 is the matrix defined by (15). Clearly

$$\{1, e^{i(\omega_1+\omega_2)}, e^{-i\omega_1}, e^{-i\omega_2}\}$$

has 3-fold rotational symmetry and it could be used as the initial symmetric filter bank, while both

$$\mathrm{diag}(1, e^{i(\omega_1+\omega_2)}, e^{-i\omega_1}, e^{-i\omega_2})$$

and

$$\mathrm{diag}(1, e^{-i(\omega_1+\omega_2)}, e^{i\omega_1}, e^{i\omega_2})$$

satisfy (16) and they could be used to build the block matrices. Next we use

$$A(\omega) = A\ \mathrm{diag}(1, e^{i(\omega_1+\omega_2)}, e^{-i\omega_1}, e^{-i\omega_2}) \tag{17}$$

and

$$A(\omega) = A\ \mathrm{diag}(1, e^{-i(\omega_1+\omega_2)}, e^{i\omega_1}, e^{i\omega_2}) \tag{18}$$

as the block matrices, where A is a 4×4 (real) constant matrix. One can verify that for $A(\omega)$ defined by (17) or by (18), $A(\omega)$ satisfies (16) if and only if A has the form:

$$A = \begin{bmatrix} a_{11} & a_{12} & a_{12} & a_{12} \\ a_{21} & a_{22} & a_{23} & a_{24} \\ a_{21} & a_{24} & a_{22} & a_{23} \\ a_{21} & a_{23} & a_{24} & a_{22} \end{bmatrix}. \tag{19}$$

Based on the above discussion, we reach the following result on the filter banks with 3-fold rotational symmetry.

Theorem 1: If $\{p, q^{(1)}, q^{(2)}, q^{(3)}\}$ is given by

$$\begin{bmatrix} p(\omega) \\ q^{(1)}(\omega) \\ q^{(2)}(\omega) \\ q^{(3)}(\omega) \end{bmatrix} = \frac{1}{2} A_n(2\omega) \cdots A_1(2\omega) A_0 \begin{bmatrix} 1 \\ e^{i(\omega_1+\omega_2)} \\ e^{-i\omega_1} \\ e^{-i\omega_2} \end{bmatrix} \tag{20}$$

for some $n \in \mathbf{Z}_+$, where A_0 is a constant matrix of the form (19), and each $A_k(\omega)$ is given by (17) or (18) with A being a constant matrix A_k of the form (19), then $\{p(\omega), q^{(1)}(\omega), q^{(2)}(\omega), q^{(3)}(\omega)\}$ is an FIR filter bank with 3-fold rotational symmetry.

In the next two subsections, we show that the block structure in (20) will yield orthogonal and biorthogonal FIR filter banks with 3-fold rotational symmetry.

B. Orthogonal filter banks with 3-fold rotational symmetry

In this subsection, we provide a block structure of orthogonal filter banks with 3-fold rotational symmetry. For an FIR filter bank $\{p, q^{(1)}, q^{(2)}, q^{(3)}\}$, denote

$$U(\omega) = \begin{bmatrix} p(\omega) & p(\omega+\eta_1) & p(\omega+\eta_2) & p(\omega+\eta_3) \\ q^{(1)}(\omega) & q^{(1)}(\omega+\eta_1) & q^{(1)}(\omega+\eta_2) & q^{(1)}(\omega+\eta_3) \\ q^{(2)}(\omega) & q^{(2)}(\omega+\eta_1) & q^{(2)}(\omega+\eta_2) & q^{(2)}(\omega+\eta_3) \\ q^{(3)}(\omega) & q^{(3)}(\omega+\eta_1) & q^{(3)}(\omega+\eta_2) & q^{(3)}(\omega+\eta_3) \end{bmatrix},$$

where η_1, η_2, η_3 are given in (10). Then $\{p, q^{(1)}, q^{(2)}, q^{(3)}\}$ is orthogonal if and only if $U(\omega)$ satisfies

$$U(\omega)U(\omega)^* = I_4, \quad \omega \in \mathbb{R}^2. \tag{21}$$

Write $p(\omega), q^{(1)}(\omega), q^{(2)}(\omega), q^{(3)}(\omega)$ as

$$p(\omega) = \frac{1}{2}\Big(p_{ee}(2\omega) + p_{oo}(2\omega)e^{i(\omega_1+\omega_2)} + p_{oe}(2\omega)e^{-i\omega_1} + p_{eo}(2\omega)e^{-i\omega_2}\Big),$$

$$q^{(\ell)}(\omega) = \frac{1}{2}\Big(q_{ee}^{(\ell)}(2\omega) + q_{oo}^{(\ell)}(2\omega)e^{i(\omega_1+\omega_2)} + q_{oe}^{(\ell)}(2\omega)e^{-i\omega_1} + q_{eo}^{(\ell)}(2\omega)e^{-i\omega_2}\Big),\ 1 \le \ell \le 3.$$

Let $V(\omega)$ denote the polyphase matrix of $\{p(\omega), q^{(1)}(\omega), q^{(2)}(\omega), q^{(3)}(\omega)\}$:

$$V(\omega) = \begin{bmatrix} p_{ee}(\omega) & p_{oo}(\omega) & p_{oe}(\omega) & p_{eo}(\omega) \\ q_{ee}^{(1)}(\omega) & q_{oo}^{(1)}(\omega) & q_{oe}^{(1)}(\omega) & q_{eo}^{(1)}(\omega) \\ q_{ee}^{(2)}(\omega) & q_{oo}^{(2)}(\omega) & q_{oe}^{(2)}(\omega) & q_{eo}^{(2)}(\omega) \\ q_{ee}^{(3)}(\omega) & q_{oo}^{(3)}(\omega) & q_{oe}^{(3)}(\omega) & q_{eo}^{(3)}(\omega) \end{bmatrix}. \tag{22}$$

Clearly,

$$[p(\omega), q^{(1)}(\omega), q^{(2)}(\omega), q^{(3)}(\omega)]^T = \frac{1}{2}V(2\omega)[1, e^{i(\omega_1+\omega_2)}, e^{-i\omega_1}, e^{-i\omega_2}]^T,$$

and one can show that (21) is equivalent to

$$V(\omega)V(\omega)^* = I_4, \quad \omega \in \mathbb{R}^2. \tag{23}$$

Therefore, to construct orthogonal $\{p, q^{(1)}, q^{(2)}, q^{(3)}\}$, we need only to construct $V(\omega)$ such that it satisfies (23).

If $\{p, q^{(1)}, q^{(2)}, q^{(3)}\}$ is given by (20), then $V(\omega) = A_n(\omega)A_{n-1}(\omega)\cdots A_1(\omega)A_0$. Furthermore, if the constant matrices $A_k, 0 \le k \le n$, are orthogonal, then $V(\omega)$ satisfies (23). One can obtain that if a constant matrix A_k of the form (19) is orthogonal, then it can be written as $\mathrm{diag}(s_1, s_2, s_2, s_2)C_k\mathrm{diag}(s_3, s_4, s_4, s_4)$, where $s_\ell = \pm 1, 1 \le \ell \le 4$, and

$$C_k = \begin{bmatrix} \alpha_k & \beta_k & \beta_k & \beta_k \\ \beta_k & \gamma_k & \eta_k & \zeta_k \\ \beta_k & \zeta_k & \gamma_k & \eta_k \\ \beta_k & \eta_k & \zeta_k & \gamma_k \end{bmatrix}, \tag{24}$$

with

$$\alpha_k = \frac{3t_k^2 - 1}{1 + 3t_k^2},\ \beta_k = \frac{2t_k}{1 + 3t_k^2},\ \gamma_k = -\alpha_k - \eta_k - \zeta_k,$$
$$\eta_k = \frac{1}{2}(-\zeta_k - \alpha_k \pm \sqrt{\alpha_k^2 + 4\beta_k^2 - 3\zeta_k^2 - 2\zeta_k\alpha_k}). \tag{25}$$

Thus an orthogonal matrix C_k of the form (19) is given by two free parameters t_k and ζ_k.

Theorem 2: If $\{p, q^{(1)}, q^{(2)}, q^{(3)}\}$ is given by (20), where each $A_k(\omega)$ is given by (17) or (18) with A being $\mathrm{diag}(s_1, s_2, s_2, s_2)C_k\mathrm{diag}(s_3, s_4, s_4, s_4)$ for some C_k given in (24), then $\{p, q^{(1)}, q^{(2)}, q^{(3)}\}$ is an orthogonal FIR filter bank with 3-fold rotational symmetry.

Transforming $\{p, q^{(1)}, q^{(2)}, q^{(3)}\}$ given in Theorem 2 with the matrix U to filter banks on the hexagonal lattice, we have a family of orthogonal FIR hexagonal filter banks with 3-fold rotational symmetry given by a block structure. For this family of orthogonal filter banks given by free parameters $t_k, \zeta_k, 0 \le k \le n$, one can design the filters with desirable properties for one's specific applications. Here we consider the filters based on the smoothness of the associated scaling functions ϕ. Next we consider two examples based on this structure.

Example 1: Let $\{p, q^{(1)}, q^{(2)}, q^{(3)}\}$ be the orthogonal filter bank with 3-fold rotational symmetry given by

$$C_1\mathrm{diag}(1, e^{-2i(\omega_1+\omega_2)}, e^{2i\omega_1}, e^{2i\omega_2})C_0 \begin{bmatrix} 1 \\ e^{i(\omega_1+\omega_2)} \\ e^{-i\omega_1} \\ e^{-i\omega_2} \end{bmatrix}, \tag{26}$$

where C_0 and C_1 are given by (24) for some $t_0, \zeta_0, t_1, \zeta_1$. The lowpass filter $p(\omega)$ is given by three free parameters t_0, ζ_0 and t_1. With the choice of $+$ in $\pm$ for η_0 in (25), and

$$t_0 = \frac{2 + \sqrt{13}}{3},\ \zeta_0 = \frac{5 - \sqrt{13}}{24}, t_1 = -\frac{4 + \sqrt{13}}{3},$$

the corresponding $p(\omega)$ has sum rule order 2, and the scaling function ϕ is in $W^{0.9425}(\mathbb{R}^2)$. For $p(\omega)$ given by (26), the maximum order of sum rules it can have is 2. From the numerical calculations, we also find that 0.94254 is almost the highest Sobolev smoothness order ϕ can gain.

Example 2: Let $\{p, q^{(1)}, q^{(2)}, q^{(3)}\}$ be the orthogonal filter bank with 3-fold rotational symmetry given by

$$C_2\mathrm{diag}(1, e^{2i(\omega_1+\omega_2)}, e^{-2i\omega_1}, e^{-2i\omega_2}) \cdot$$
$$C_1\mathrm{diag}(1, e^{-2i(\omega_1+\omega_2)}, e^{2i\omega_1}, e^{2i\omega_2}) \cdot$$
$$C_0[1, e^{i(\omega_1+\omega_2)}, e^{-i\omega_1}, e^{-i\omega_2}]^T,$$

where C_0, C_1, C_2 are matrices defined by (17) with free parameters $t_k, \zeta_k, k = 0, 1, 2$. With the choice $+$ in $\pm$ for η_k in (25), and

$$t_0 = 2.22285908185090,\ \zeta_0 = 0.02319874938139,$$
$$t_1 = 0.18471231877448,\ \zeta_1 = 0.60189976981183,$$
$$t_2 = 0.04160159358460$$

(ζ_2 is a free parameter), we get the smoothest ϕ with $\phi \in W^{1.1388}(\mathbb{R}^2)$.

We have considered orthogonal filters with more non-zero impulse response coefficients by using more blocks $A_k(\omega)$ in (20). Unfortunately, in term of the smoothness of the scaling functions, using a few more blocks $A_k(\omega)$ does not yield orthogonal scaling functions with significantly higher smoothness order. In the next section, we consider 3-fold rotational symmetric biorthogonal filter banks, which give us more flexility for the construction of perfect reconstruction filter banks.

C. Biorthogonal filter banks with 3-fold rotational symmetry

Let $\{p, q^{(1)}, q^{(2)}, q^{(3)}\}$ and $\{\tilde{p}, \tilde{q}^{(1)}, \tilde{q}^{(2)}, \tilde{q}^{(3)}\}$ be two filter banks, $V(\omega)$ and $\widetilde{V}(\omega)$ be their polyphase matrices defined by (22). Then one can shows as in §III.B that $\{p, q^{(1)}, q^{(2)}, q^{(3)}\}$ and $\{\tilde{p}, \tilde{q}^{(1)}, \tilde{q}^{(2)}, \tilde{q}^{(3)}\}$ are biorthogonal to each other if and only if $V(\omega)$ and $\widetilde{V}(\omega)$ satisfy

$$V(\omega)\widetilde{V}(\omega)^* = I_4,\ \omega \in \mathbb{R}^2.$$

If $\{p, q^{(1)}, q^{(2)}, q^{(3)}\}$ is the FIR filter bank given by (20) with $A_k(\omega)$ given by (17) or (18) for A to be some 4×4 real matrix A_k, then $V(\omega) = A_n(\omega)A_{n-1}(\omega)\cdots A_1(\omega)A_0$. Suppose $A_k, 0 \le k \le n$ are nonsingular. Then $(V(\omega)^*)^{-1} = \tilde{A}_n(\omega)\tilde{A}_{n-1}(\omega)\cdots\tilde{A}_1(\omega)\tilde{A}_0$ with $\tilde{A}_0 = A_0^{-T}$ and

$$\tilde{A}_k(\omega) = A_k^{-T}(1, e^{i(\omega_1+\omega_2)}, e^{-i\omega_1}, e^{-i\omega_2}) \tag{27}$$

or

$$\tilde{A}_k(\omega) = A_k^{-T}(1, e^{-i(\omega_1+\omega_2)}, e^{i\omega_1}, e^{i\omega_2}). \tag{28}$$

One can easily show that if A_k has the form of (19), then so dose A_k^{-T}. Thus, by Proposition 1, $\{\tilde{p}, \tilde{q}^{(1)}, \tilde{q}^{(2)}, \tilde{q}^{(3)}\}$ with its polyphase matrix $\widetilde{V}(\omega) = (V(\omega)^*)^{-1}$ also has 3-fold rotational symmetry. Therefore, we have the following result.

Theorem 3: Let $\{p, q^{(1)}, q^{(2)}, q^{(3)}\}$ be the FIR filter bank given by (20) with

$$A_k(\omega) = A_k(1, e^{i(\omega_1+\omega_2)}, e^{-i\omega_1}, e^{-i\omega_2}) \tag{29}$$

or

$$A_k(\omega) = A_k(1, e^{-i(\omega_1+\omega_2)}, e^{i\omega_1}, e^{i\omega_2}), \tag{30}$$

where $A_k, 0 \le k \le n$ are 4×4 nonsingular real matrices of the form (19). Suppose $\{\tilde{p}, \tilde{q}^{(1)}, \tilde{q}^{(2)}, \tilde{q}^{(3)}\}$ is given by

$$\begin{bmatrix} \tilde{p}(\omega) \\ \tilde{q}^{(1)}(\omega) \\ \tilde{q}^{(2)}(\omega) \\ \tilde{q}^{(3)}(\omega) \end{bmatrix} = \frac{1}{2}\tilde{A}_n(2\omega)\cdots\tilde{A}_1(2\omega)\tilde{A}_0 \begin{bmatrix} 1 \\ e^{i(\omega_1+\omega_2)} \\ e^{-i\omega_1} \\ e^{-i\omega_2} \end{bmatrix}, \tag{31}$$

where $\tilde{A}_0 = A_0^{-T}$, $\tilde{A}_k(\omega)$ is given by (27) (if $A_k(\omega)$ is given by (29)) or by (28) (if $A_k(\omega)$ is given by (30)).

Then $\{\tilde{p}, \tilde{q}^{(1)}, \tilde{q}^{(2)}, \tilde{q}^{(3)}\}$ is an FIR filter bank biorthogonal to $\{p, q^{(1)}, q^{(2)}, q^{(3)}\}$ and it has 3-fold rotational symmetry.

Theorem 3 provides a family of biorthogonal FIR filter banks with 3-fold rotational symmetry. Compared with the orthogonal filter banks given in Theorem 2, this family of biorthogonal filter banks has more flexibility for the design of desired filters.

Example 3: Let $\{p, q^{(1)}, q^{(2)}, q^{(3)}\}$ and $\{\tilde{p}, \tilde{q}^{(1)}, \tilde{q}^{(2)}, \tilde{q}^{(3)}\}$ be the biorthogonal filter banks with 3-fold rotational symmetry given by Theorem 3 with $n = 1$, namely,

$$\begin{aligned}
&[p(\omega), q^{(1)}(\omega), q^{(2)}(\omega), q^{(3)}(\omega)]^T = \\
&\quad A_1 \mathrm{diag}(1, e^{-2i(\omega_1+\omega_2)}, e^{2i\omega_1}, e^{2i\omega_2}) \cdot \\
&\quad A_0 [1, e^{i(\omega_1+\omega_2)}, e^{-i\omega_1}, e^{-i\omega_2}]^T, \\
&[\tilde{p}(\omega), \tilde{q}^{(1)}(\omega), \tilde{q}^{(2)}(\omega), \tilde{q}^{(3)}(\omega)]^T = \\
&\quad A_1^{-T} \mathrm{diag}(1, e^{-2i(\omega_1+\omega_2)}, e^{2i\omega_1}, e^{2i\omega_2}) \cdot \\
&\quad A_0^{-T} [1, e^{i(\omega_1+\omega_2)}, e^{-i\omega_1}, e^{-i\omega_2}]^T,
\end{aligned}$$

where A_0 and A_1 are nonsingular matrices of the form (19). We can choose the free parameters for A_0 and A_1 such that the resulting scaling functions $\phi \in W^{1.1860}(\mathbb{R}^2), \tilde{\phi} \in W^{0.5212}(\mathbb{R}^2)$ and the lowpass filters $p(\omega)$ and $\tilde{p}(\omega)$ have sum rules of order 2 and order 1 respectively. Since smoothness order of the scaling functions is still low, the selected parameters are not provided here.

Here and in the next example, we intently construct the scaling functions with one smoother than the other so that one filter bank can be used as the analysis filter bank and the other can be used as the synthesis filter bank which requires smoother scaling function and wavelets.

Example 4: Let $\{p, q^{(1)}, q^{(2)}, q^{(3)}\}$ and $\{\tilde{p}, \tilde{q}^{(1)}, \tilde{q}^{(2)}, \tilde{q}^{(3)}\}$ be the biorthogonal filter banks with 3-fold rotational symmetry given by Theorem 3 with $n = 2$:

$$\begin{aligned}
&[p(\omega), q^{(1)}(\omega), q^{(2)}(\omega), q^{(3)}(\omega)]^T = \\
&\quad A_2 \mathrm{diag}(1, e^{2i(\omega_1+\omega_2)}, e^{-2i\omega_1}, e^{-2i\omega_2}) \cdot \\
&\quad A_1 \mathrm{diag}(1, e^{-2i(\omega_1+\omega_2)}, e^{2i\omega_1}, e^{2i\omega_2}) \cdot \\
&\quad A_0 [1, e^{i(\omega_1+\omega_2)}, e^{-i\omega_1}, e^{-i\omega_2}]^T, \\
&[\tilde{p}(\omega), \tilde{q}^{(1)}(\omega), \tilde{q}^{(2)}(\omega), \tilde{q}^{(3)}(\omega)]^T = \\
&\quad A_2^{-T} \mathrm{diag}(1, e^{2i(\omega_1+\omega_2)}, e^{-2i\omega_1}, e^{-2i\omega_2}) \cdot \\
&\quad A_1^{-T} \mathrm{diag}(1, e^{-2i(\omega_1+\omega_2)}, e^{2i\omega_1}, e^{2i\omega_2}) \cdot \\
&\quad A_0^{-T} [1, e^{i(\omega_1+\omega_2)}, e^{-i\omega_1}, e^{-i\omega_2}]^T,
\end{aligned}$$

where A_0, A_1 and A_2 are nonsingular matrices of the form (19). In this case, we can select the free parameters for A_0, A_1 and A_2 such that the resulting scaling functions $\phi \in W^{1.5294}(\mathbb{R}^2), \tilde{\phi} \in W^{0.3859}(\mathbb{R}^2)$ and the lowpass filters $p(\omega)$ and $\tilde{p}(\omega)$ have sum rules of order 2 and order 1 respectively. The selected parameters are provided in Appendix A.

IV. Orthogonal and biorthogonal FIR filter banks with 3-fold axial symmetry

In this section we study the construction of orthogonal and biorthogonal filter banks with 3-fold axial symmetry. The 3-fold axial symmetry of filter banks is discussed in §VI.A, and block structures of orthogonal and biorthogonal FIR filter banks with 3-fold axial symmetry are presented in §VI.B and §VI.C, respectively.

A. FIR filter banks with 3-fold axial symmetry

Let $\{p, q^{(1)}, q^{(2)}, q^{(3)}\}$ be an FIR filter bank. Then it has 3-fold axial symmetry, that is it satisfies (9), if and only if

$$\begin{cases} p(\omega) = p(N_e\omega) = p(W^{-T}\omega) = p({S_e}^{-T}\omega), \\ q^{(1)}(\omega) = q^{(1)}(N_e\omega) = q^{(2)}(R_1^T\omega) = q^{(3)}(R_2^T\omega). \end{cases} \tag{32}$$

Before we derive a block structure of filter banks with 3-fold axial symmetry, we first have the following proposition about the 3-fold axial symmetry property of a filter bank.

Proposition 3: A filter bank $\{p, q^{(1)}, q^{(2)}, q^{(3)}\}$ has 3-fold axial symmetry if and only if it satisfies

$$\left[p,\ q^{(1)},\ q^{(2)},\ q^{(3)}\right]^T (N_e\omega) = M_1 \left[p(\omega),\ q^{(1)}(\omega),\ q^{(2)}(\omega),\ q^{(3)}(\omega)\right]^T, \tag{33}$$

$$\left[p,\ q^{(1)},\ q^{(2)},\ q^{(3)}\right]^T (W^{-T}\omega) = M_2 \left[p(\omega),\ q^{(1)}(\omega),\ q^{(2)}(\omega),\ q^{(3)}(\omega)\right]^T, \tag{34}$$

$$\left[p,\ q^{(1)},\ q^{(2)},\ q^{(3)}\right]^T ({S_e}^{-T}\omega) = M_3 \left[p(\omega),\ q^{(1)}(\omega),\ q^{(2)}(\omega),\ q^{(3)}(\omega)\right]^T, \tag{35}$$

where

$$M_1 = \begin{bmatrix} 1 & 0 & 0 & 0 \\ 0 & 1 & 0 & 0 \\ 0 & 0 & 0 & 1 \\ 0 & 0 & 1 & 0 \end{bmatrix},\ M_2 = \begin{bmatrix} 1 & 0 & 0 & 0 \\ 0 & 0 & 0 & 1 \\ 0 & 0 & 1 & 0 \\ 0 & 1 & 0 & 0 \end{bmatrix},$$
$$M_3 = \begin{bmatrix} 1 & 0 & 0 & 0 \\ 0 & 0 & 1 & 0 \\ 0 & 1 & 0 & 0 \\ 0 & 0 & 0 & 1 \end{bmatrix}. \tag{36}$$

The proof of Proposition 3 is given in Appendix B. Next, we consider the filter bank $\{p, q^{(1)}, q^{(2)}, q^{(3)}\}$ which can be given by the product of block matrices. Assume that $[p(\omega), q^{(1)}(\omega), q^{(2)}(\omega), q^{(3)}(\omega)]^T$ can be written as $B(2\omega)[p_0(\omega), q_0^{(1)}(\omega), q_0^{(2)}(\omega), q_0^{(3)}(\omega)]^T$, where $B(\omega)$ is a 4×4 matrix with trigonometric polynomial entries and $\{p_0, q_0^{(1)}, q_0^{(2)}, q_0^{(3)}\}$ is another FIR filter bank. If both $\{p, q^{(1)}, q^{(2)}, q^{(3)}\}$ and $\{p_0, q_0^{(1)}, q_0^{(2)}, q_0^{(3)}\}$ have 3-fold axial symmetry, then Proposition 3 implies that $B(\omega)$ satisfies

$$\begin{cases} B(N_e\omega) = M_1 B(\omega) M_1,\ B(W^{-T}\omega) = M_2 B(\omega) M_2, \\ B({S_e}^{-T}\omega) = M_3 B(\omega) M_3, \end{cases} \tag{37}$$

where M_1, M_2 and M_3 are the matrices defined by (36). Since both $\mathrm{diag}(1, e^{i(\omega_1+\omega_2)}, e^{-i\omega_1}, e^{-i\omega_2})$ and $\mathrm{diag}(1, e^{-i(\omega_1+\omega_2)}, e^{i\omega_1}, e^{i\omega_2})$ satisfy (37), they could be used to build the block matrices. Next we will use

$$B(\omega) = B\ \mathrm{diag}(1, e^{i(\omega_1+\omega_2)}, e^{-i\omega_1}, e^{-i\omega_2}) \tag{38}$$

and

$$B(\omega) = B\ \mathrm{diag}(1, e^{-i(\omega_1+\omega_2)}, e^{i\omega_1}, e^{i\omega_2}) \tag{39}$$

as the block matrices, where B is a 4×4 (real) constant matrix. One can verify that for $B(\omega)$ defined by (38) or by (39), $B(\omega)$ satisfies (37) if and only if B has the form:

$$B = \begin{bmatrix} b_{11} & b_{12} & b_{12} & b_{12} \\ b_{21} & b_{22} & b_{23} & b_{23} \\ b_{21} & b_{23} & b_{22} & b_{23} \\ b_{21} & b_{23} & b_{23} & b_{22} \end{bmatrix}. \tag{40}$$

Based on the above discussion, we reach the following theorem on the filter banks with 3-fold axial symmetry.

Theorem 4: If $\{p, q^{(1)}, q^{(2)}, q^{(3)}\}$ is given by

$$\begin{bmatrix} p(\omega) \\ q^{(1)}(\omega) \\ q^{(2)}(\omega) \\ q^{(3)}(\omega) \end{bmatrix} = \frac{1}{2} B_n(2\omega)\cdots B_1(2\omega)B_0 \begin{bmatrix} 1 \\ e^{i(\omega_1+\omega_2)} \\ e^{-i\omega_1} \\ e^{-i\omega_2} \end{bmatrix} \tag{41}$$

for some $n \in \mathbf{Z}_+$, where B_0 is a 4×4 constant matrix of the form (40), each $B_k(\omega)$ is given by (38) or (39) for some 4×4 constant matrix B_k of the form (40), then $\{p, q^{(1)}, q^{(2)}, q^{(3)}\}$ has 3-fold axial symmetry.

B. Allen's orthogonal filter banks

In this subsection, we show that the block structure in (41) will yield 3-fold axial symmetric orthogonal FIR filter banks, which were studied in [4], [26]. For an FIR filter bank $\{p, q^{(1)}, q^{(2)}, q^{(3)}\}$, let $V(\omega)$ denote its polyphase matrix defined in (22). If $\{p, q^{(1)}, q^{(2)}, q^{(3)}\}$ is given by (41), then $V(\omega) = B_n(\omega)B_{n-1}(\omega)\cdots B_1(\omega)B_0$. Thus, if the constant matrices B_k are orthogonal, then $V(\omega)$ satisfies (23), and hence, (41) gives a family of orthogonal filter banks. One can check that if a constant matrix B_k of the form (40) is orthogonal, then it can be written as (refer to [4])

$$B_k = \frac{1}{1+3b_k^2}\begin{bmatrix} 3b_k^2-1 & 2b_k & 2b_k & 2b_k \\ 2b_k & 1+b_k^2 & -2b_k^2 & -2b_k^2 \\ 2b_k & -2b_k^2 & 1+b_k^2 & -2b_k^2 \\ 2b_k & -2b_k^2 & -2b_k^2 & 1+b_k^2 \end{bmatrix} \tag{42}$$

or it can be written as

$$B_k = \frac{1}{1+3b_k^2}\cdot \begin{bmatrix} \pm(1-3b_k^2) & 2b_k & 2b_k & 2b_k \\ \pm 2b_k & -(1+b_k^2) & 2b_k^2 & 2b_k^2 \\ \pm 2b_k & 2b_k^2 & -(1+b_k^2) & 2b_k^2 \\ \pm 2b_k & 2b_k^2 & 2b_k^2 & -(1+b_k^2) \end{bmatrix} \tag{43}$$

with $b_k \in \mathbb{R}$.

Theorem 5: If $\{p, q^{(1)}, q^{(2)}, q^{(3)}\}$ is given by (41) with

$$B_k(\omega) = B_k \mathrm{diag}(1, e^{i(\omega_1+\omega_2)}, e^{-i\omega_1}, e^{-i\omega_2}),$$

or

$$B_k(\omega) = B_k \mathrm{diag}(1, e^{-i(\omega_1+\omega_2)}, e^{i\omega_1}, e^{i\omega_2}),$$

where $B_k, 0 \le k \le n$ are given by (42) or (43), then $\{p, q^{(1)}, q^{(2)}, q^{(3)}\}$ is an orthogonal filter bank with 3-fold axial symmetry.

Transforming $\{p, q^{(1)}, q^{(2)}, q^{(3)}\}$ given in Theorem 5 with the matrix U to hexagonal filter banks, we have a family of orthogonal hexagonal filter banks with 3-fold axial symmetry given by a block structure. This structure is the one given by Allen in [4], and it is referred here as Allen's structure. [4] and [26] constructed several orthogonal filter banks based on the compaction of filters. Here we consider the filters based on the smoothness of the associated scaling functions.

Example 5: Let $\{p(\omega), q^{(1)}(\omega), q^{(2)}(\omega), q^{(3)}(\omega)\}$ be the orthogonal filter bank given by

$$B_1 \mathrm{diag}(1, e^{-2i(\omega_1+\omega_2)}, e^{2i\omega_1}, e^{2i\omega_2}) B_0 \begin{bmatrix} 1 \\ e^{i(\omega_1+\omega_2)} \\ e^{-i\omega_1} \\ e^{-i\omega_2} \end{bmatrix}, \tag{44}$$

with B_0, B_1 given by (42) for some $b_0, b_1 \in \mathbb{R}$. The hexagonal filter bank corresponding to this filter bank is called the L-Trigon of the R-Trigon in [4]. One can show that with the choices of

$$b_0 = \frac{1}{9}(2-\sqrt{13}), \quad b_1 = \frac{1}{3}(4-\sqrt{13}),$$

the resulting lowpass filter $p(\omega)$ has sum rule order 2, and the scaling function ϕ is in $W^{0.9425}(\mathbb{R}^2)$. Actually, this resulting $p(\omega)$ is the lowpass filter of sum rule order 2 in Example 1. The non-zero impulse response coefficients $p_{\mathbf{k}}, q_{\mathbf{k}}^{(\ell)}$ of the filters are

$$\begin{aligned}
&p_{00} = \frac{13+3\sqrt{13}}{16}, \quad p_{10} = p_{01} = p_{-1-1} = \frac{13-\sqrt{13}}{16}, \\
&p_{11} = p_{0-1} = p_{-10} = \frac{19+\sqrt{13}}{48}, \\
&p_{22} = p_{0-2} = p_{-20} = \frac{1-\sqrt{13}}{16}, \\
&p_{23} = p_{32} = p_{1-2} = p_{-21} = p_{-1-3} = p_{-3-1} = \frac{-5+\sqrt{13}}{48}, \\
&q_{00}^{(1)} = -\frac{3+\sqrt{13}}{16}, \; q_{11}^{(1)} = \frac{55+9\sqrt{13}}{48}, \\
&q_{10}^{(1)} = q_{01}^{(1)} = q_{-1-1}^{(1)} = \frac{1-\sqrt{13}}{16}, \\
&q_{0-1}^{(1)} = q_{-10}^{(1)} = \frac{-21+5\sqrt{13}}{48}, \; q_{22}^{(1)} = -\frac{5+7\sqrt{13}}{48}, \\
&q_{0-2}^{(1)} = q_{-20}^{(1)} = \frac{-17+5\sqrt{13}}{48}, \\
&q_{32}^{(1)} = q_{23}^{(1)} = \frac{-9+\sqrt{13}}{48}, \\
&q_{1-2}^{(1)} = q_{-21}^{(1)} = q_{-1-3}^{(1)} = q_{-3-1}^{(1)} = \frac{11-3\sqrt{13}}{48},
\end{aligned}$$

and $q_{\mathbf{k}}^{(2)}$, $q_{\mathbf{k}}^{(3)}$ are given by (8).

We have also considered orthogonal filters with more non-zero impulse response coefficients by using more blocks $B_k(\omega)$ in (41). Again, we find that using a few more blocks $B_k(\omega)$ does not yield orthogonal scaling functions with significantly higher smoothness order.

Let $\{p, q^{(1)}, q^{(2)}, q^{(3)}\}$ be the FIR filter bank given by (41) with $B_k(\omega) = B_k \mathrm{diag}(1, z_1^{-1}z_2^{-1}, z_1, z_2)$ (or $B_k(\omega) = B_k \mathrm{diag}(1, z_1 z_2, z_1^{-1}, z_2^{-1})$), where $B_k, 0 \le k \le n$ are 4×4 nonsingular constant real matrices of the form (40), and z_1, z_2

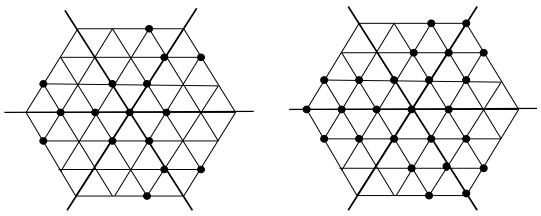

Fig. 4. *Non-zero impulse response coefficients of filters with Allen's structure (left) and those with new structure (right)*

are defined by (1). Then $\{\tilde{p}(\omega), \tilde{q}^{(1)}(\omega), \tilde{q}^{(2)}(\omega), \tilde{q}^{(3)}(\omega)\}$ given by

$$\frac{1}{2}\tilde{B}_n(2\omega)\cdots\tilde{B}_1(2\omega)B_0^{-T}[1, z_1^{-1}z_2^{-1}, z_1, z_2]^T,$$

where $\tilde{B}_k(\omega) = B_k^{-T}\mathrm{diag}(1, z_1^{-1}z_2^{-1}, z_1, z_2)$ (or $\tilde{B}_k(\omega) = B_k^{-T}\mathrm{diag}(1, z_1z_2, z_1^{-1}, z_2^{-1})$ correspondingly), is biorthogonal to $\{p, q^{(1)}, q^{(2)}, q^{(3)}\}$ and it has 3-fold axial symmetry. Therefore, by choosing nonsingular matrices B_k of the form (40), one has a family of biorthogonal FIR filter banks given by free parameters. Compared with the orthogonal filter banks of 3-fold axial symmetry given in Theorem 5, these biorthogonal filter banks give us more flexibility for the design of desired filters. However, in terms of the smoothness of the scaling functions ϕ and $\tilde{\phi}$, they do not yield smooth $\phi, \tilde{\phi}$ with reasonable supports. Because of this, we introduce in the next subsection another family of biorthogonal filter banks with 3-fold axial symmetry.

C. Biorthogonal filter banks with 3-fold axial symmetry

In this subsection we introduce another family of biorthogonal filter banks with 3-fold axial symmetry which is based on the following block matrix:

$$D(\omega) = \frac{1}{2}\begin{bmatrix} a & b+cz_1z_2 & b+cz_1^{-1} & b+cz_2^{-1} \\ t_1 & t_5+t_3z_1z_2 & t_2+t_4z_1^{-1} & t_2+t_4z_2^{-1} \\ t_1 & t_2+t_4z_1z_2 & t_5+t_3z_1^{-1} & t_2+t_4z_2^{-1} \\ t_1 & t_2+t_4z_1z_2 & t_2+t_4z_1^{-1} & t_5+t_3z_2^{-1} \end{bmatrix}, \tag{45}$$

where $a, b, c, t_j, 1 \le j \le 5$, are real numbers, and z_1, z_2 are given by (1). One can verify that $D(\omega)$ satisfies (37). $D(\omega)$ yields primal filter banks $\{p, q^{(1)}, q^{(2)}, q^{(3)}\}$ with denser non-zero impulse response coefficients (and hence, they will produce smoother scaling functions and wavelets). For example, the black dots in the left part of Fig. 4 indicate the non-zero impulse response coefficients of $p(\omega)$ from $B_1(2\omega)B_0[1, e^{i\omega_1}e^{i\omega_2}, e^{-i\omega_1}, e^{-i\omega_2}]^T$, while the non-zero impulse response coefficients of $p(\omega)$ from $D_2(2\omega)D_1(2\omega)[1, e^{i\omega_1}e^{i\omega_2}, e^{-i\omega_1}, e^{-i\omega_2}]^T$ are shown in the right part of Fig. 4 as the black dots.

We can choose some special t_j such that $\det(D(\omega))$ is a constant and hence $\widetilde{D}(\omega) = (D(\omega)^*)^{-1}$ is a matrix with each entry being a (Laurent) polynomial of z_1, z_2. The possible choices are

$$t_2 = t_5 = \frac{bt_1}{a}, \tag{46}$$

or

$$t_3 = t_4 = \frac{ct_1}{a}. \tag{47}$$

In these two cases, $\det(D(\omega))$ is $\frac{1}{16}(t_3-t_4)^2(at_3+2at_4-3ct_1)$. With t_2, t_5 given in (46), $\widetilde{D}(\omega) = (D(\omega)^*)^{-1}$ is

$$\widetilde{D}(\omega) = \frac{2}{(t_3-t_4)(at_3+2at_4-3ct_1)}\cdot \begin{bmatrix} \tilde{a}-\frac{b\tilde{b}}{a}(z_1z_2+\frac{1}{z_1}+\frac{1}{z_2}) & \tilde{b}z_1z_2 & \frac{\tilde{b}}{z_1} & \frac{\tilde{b}}{z_2} \\ \tilde{e}-\frac{b}{a}(\tilde{c}z_1z_2+\frac{\tilde{d}}{z_1}+\frac{\tilde{d}}{z_2}) & \tilde{c}z_1z_2 & \frac{\tilde{d}}{z_1} & \frac{\tilde{d}}{z_2} \\ \tilde{e}-\frac{b}{a}(\tilde{d}z_1z_2+\frac{\tilde{c}}{z_1}+\frac{\tilde{d}}{z_2}) & \tilde{d}z_1z_2 & \frac{\tilde{c}}{z_1} & \frac{\tilde{d}}{z_2} \\ \tilde{e}-\frac{b}{a}(\tilde{d}z_1z_2+\frac{\tilde{d}}{z_1}+\frac{\tilde{c}}{z_2}) & \tilde{d}z_1z_2 & \frac{\tilde{d}}{z_1} & \frac{\tilde{c}}{z_2} \end{bmatrix}, \tag{48}$$

where

$$\tilde{a} = (t_3+2t_4)(t_3-t_4),\ \tilde{b} = -t_1(t_3-t_4),$$
$$\tilde{c} = at_3+at_4-2ct_1,\ \tilde{d} = ct_1-at_4,\ \tilde{e} = -c(t_3-t_4),$$

while if t_3, t_4 are given by (47), then $\widetilde{D}(\omega) = (D(\omega)^*)^{-1}$ is

$$\widetilde{D}(\omega) = \frac{2}{(t_5-t_2)(at_5+2at_2-3bt_1)}\cdot \begin{bmatrix} \tilde{a}_1-\frac{c\tilde{b}_1}{a}(z_1^{-1}z_2^{-1}+z_1+z_2) & \tilde{b}_1 & \tilde{b}_1 & \tilde{b}_1 \\ \tilde{e}_1-\frac{c}{a}(\tilde{c}_1z_1^{-1}z_2^{-1}+\tilde{d}_1z_1+\tilde{d}_1z_2) & \tilde{c}_1 & \tilde{d}_1 & \tilde{d}_1 \\ \tilde{e}_1-\frac{c}{a}(\tilde{d}_1z_1^{-1}z_2^{-1}+\tilde{c}_1z_1+\tilde{d}_1z_2) & \tilde{d}_1 & \tilde{c}_1 & \tilde{d}_1 \\ \tilde{e}_1-\frac{c}{a}(\tilde{d}_1z_1^{-1}z_2^{-1}+\tilde{d}_1z_1+\tilde{c}_1z_2) & \tilde{d}_1 & \tilde{d}_1 & \tilde{c}_1 \end{bmatrix}, \tag{49}$$

where

$$\tilde{a}_1 = (t_5+2t_2)(t_5-t_2),\ \tilde{c}_1 = at_2+at_5-2bt_1,$$
$$\tilde{b}_1 = -t_1(t_5-t_2),\ \tilde{d}_1 = bt_1-at_2,\ \tilde{e}_1 = -b(t_5-t_2).$$

Theorem 6: Let $\{p, q^{(1)}, q^{(2)}, q^{(3)}\}$ be the filter bank given by

$$\begin{bmatrix} p(\omega) \\ q^{(1)}(\omega) \\ q^{(2)}(\omega) \\ q^{(3)}(\omega) \end{bmatrix} = \frac{1}{2}D_n(\pm2\omega)\cdots D_0(\pm2\omega)\begin{bmatrix} 1 \\ e^{i(\omega_1+\omega_2)} \\ e^{-i\omega_1} \\ e^{-i\omega_2} \end{bmatrix} \tag{50}$$

for some $n \in \mathbf{Z}_+$, where $D_k(\omega), 0 \le k \le n$ are given by (45) with parameters satisfying (46) or (47). If $\{\tilde{p}, \tilde{q}^{(1)}, \tilde{q}^{(2)}, \tilde{q}^{(3)}\}$ is the filter bank given by

$$\begin{bmatrix} \tilde{p}(\omega) \\ \tilde{q}^{(1)}(\omega) \\ \tilde{q}^{(2)}(\omega) \\ \tilde{q}^{(3)}(\omega) \end{bmatrix} = \frac{1}{2}\widetilde{D}_n(\pm2\omega)\cdots\widetilde{D}_0(\pm2\omega)\begin{bmatrix} 1 \\ e^{i(\omega_1+\omega_2)} \\ e^{-i\omega_1} \\ e^{-i\omega_2} \end{bmatrix}, \tag{51}$$

where $\widetilde{D}_k(\omega) = (D_k(\omega)^*)^{-1}, 0 \le k \le n$, are given by (48) or by (49), then $\{p, q^{(1)}, q^{(2)}, q^{(3)}\}$ and $\{\tilde{p}, \tilde{q}^{(1)}, \tilde{q}^{(2)}, \tilde{q}^{(3)}\}$ are FIR filter banks with 3-fold axial symmetry and they are biorthogonal to each other.

Again, with a family of symmetric biorthogonal FIR filter banks available in Theorem 6, one can design biorthogonal filter banks for one's particular applications. Here we provide two filter banks based on the smoothness of the associated scaling functions ϕ and $\tilde{\phi}$. In the following two examples, as in Examples 3 and 4, we intently construct the scaling functions with one smoother than the other.

Example 6: Let

$$[p(\omega), q^{(1)}(\omega), q^{(2)}(\omega), q^{(3)}(\omega)]^T = \frac{1}{2} D_1(-2\omega) D_0(2\omega) [1, e^{i(\omega_1+\omega_2)}, e^{-i\omega_1}, e^{-i\omega_2}]^T,$$
$$[\tilde{p}(\omega), \tilde{q}^{(1)}(\omega), \tilde{q}^{(2)}(\omega), \tilde{q}^{(3)}(\omega)]^T = \frac{1}{2} \widetilde{D}_1(-2\omega) \widetilde{D}_0(2\omega) [1, e^{i(\omega_1+\omega_2)}, e^{-i\omega_1}, e^{-i\omega_2}]^T,$$

be the biorthogonal FIR filter banks given in Theorem 6 with $n = 1$ and the parameters satisfying (46). Then we can choose free parameters such that the resulting scaling functions $\phi \in W^{1.5105}(\mathbb{R}^2), \tilde{\phi} \in W^{0.4067}(\mathbb{R}^2)$ and the lowpass filters $p(\omega), \tilde{p}(\omega)$ have sum rules of order 2 and order 1 respectively. The impulse response coefficients of the resulting filter banks are provided in Appendix C.

Example 7: Let

$$[p(\omega), q^{(1)}(\omega), q^{(2)}(\omega), q^{(3)}(\omega)]^T = \frac{1}{2} D_2(2\omega) D_1(-2\omega) D_0(2\omega) [1, e^{i(\omega_1+\omega_2)}, e^{-i\omega_1}, e^{-i\omega_2}]^T,$$
$$[\tilde{p}(\omega), \tilde{q}^{(1)}(\omega), \tilde{q}^{(2)}(\omega), \tilde{q}^{(3)}(\omega)]^T = \frac{1}{2} \widetilde{D}_2(2\omega) \widetilde{D}_1(-2\omega) \widetilde{D}_0(2\omega) [1, e^{i(\omega_1+\omega_2)}, e^{-i\omega_1}, e^{-i\omega_2}]^T,$$

be the biorthogonal FIR filter banks given in Theorem 6 with $n = 2$ and the parameters satisfying (46). Then we can choose free parameters such that the corresponding scaling functions $\phi \in W^{1.7055}(\mathbb{R}^2), \tilde{\phi} \in W^{0.5869}(\mathbb{R}^2)$, and the lowpass filters $p(\omega), \tilde{p}(\omega)$ have sum rules of order 2 and order 1 respectively. The impulse response coefficients of these two resulting filter banks are provided in provided in Appendix D.

V. Conclusion

In this paper we obtain block structures of FIR filter banks with 3-fold rotational symmetry and FIR filter banks with 3-fold axial symmetry. These block structures yield orthogonal/biorthogonal hexagonal filter banks with 3-fold rotational symmetry and orthogonal/biorthogonal hexagonal filter banks with 3-fold axial symmetry. The construction of orthogonal and biorthogonal FIR filters with scaling functions having optimal smoothness is discussed and several orthogonal/biorthogonal filters banks are presented. Our future work is to apply these hexagonal filter banks for hexagonal image processing applications such as image enhancement and edge detection. In this paper we just consider the hexagonal filters with the dyadic refinement. In the future, we will also consider the hexagonal filters with the $\sqrt{3}$ and $\sqrt{7}$ refinements and study the construction of idealized hexagonal tight frame filter banks which contain the "idealized" highpass filters with nice frequency localizations.

Appendix A

Selected parameters in Example 4: selected a_{ij} for A_0 are

$$a_{11} = 0.53418431122656, a_{12} = 0.26151738104791,$$
$$a_{21} = 0.01459363514388, a_{22} = 1.24160756693777,$$
$$a_{23} = 0.03247147746833, a_{24} = 0.03247589636386;$$

select parameters a_{ij} for A_1 are

$$a_{11} = 1.74210812926244, a_{12} = 0.41721745109326,$$
$$a_{21} = -2.18192416765921, a_{22} = 2.51403080377387,$$
$$a_{23} = 0.55679974918931, a_{24} = 0.55661861238169;$$

and select parameters a_{ij} for A_2 are

$$a_{11} = 0.51226668946537, a_{12} = -0.00417155767962,$$
$$a_{21} = -0.83390119661419, a_{22} = -0.33354163795606,$$
$$a_{23} = 1.76565003212551, a_{24} = 0.28836976159098.$$

Appendix B

Proof of Proposition 3. Using $R_1 = WN_e$, $R_2 = S_eN_e$, one can easily show that (33)-(35) imply (32). On the other hand, using the following facts (i)-(v) about relationship among the matrices N_e, W, S_e, R_1 and R_2, one can show that (32) leads to (33)-(35):

(i). $N_e = R_1^T N_e R_2^{-T}$; (ii). $R_2^{-T} = N_e W^{-T}$;
(iii). $R_1^{-T} = N_e {S_e}^{-T}$; (iv). $R_1^{-T} W^{-T} = N_e R_1^{-T}$;
(v). $R_2^{-T} W^{-T} = N_e R_2^{-T}$.

Here we just show the formulas in (33)-(35) for $q^{(2)}$. The proof of other formulas in (33)-(35) for $p, q^{(1)}$ and $q^{(3)}$ is similar. For $q^{(2)}$, we have

$$q^{(2)}(N_e\omega) = q^{(1)}(R_1^{-T} N_e \omega)$$
$$= q^{(1)}(N_e R_2^{-T}\omega)(\text{by (i)}) = q^{(1)}(R_2^{-T}\omega) = q^{(3)}(\omega);$$
$$q^{(2)}(W^{-T}\omega) = q^{(1)}(R_1^{-T} W^{-T}\omega)$$
$$= q^{(1)}(N_e R_1^{-T}\omega)(\text{by (iv)}) = q^{(1)}(R_1^{-T}\omega) = q^{(2)}(\omega);$$
$$q^{(2)}({S_e}^{-T}\omega) = q^{(1)}(R_1^{-T} {S_e}^{-T}\omega)$$
$$= q^{(1)}(N_e R_2^{-T}\omega)(\text{by (iii)}) = q^{(1)}(R_2^{-T}\omega) = q^{(3)}(\omega),$$

as desired.

Appendix C

The biorthogonal filters in Example 5 with $\phi \in W^{1.5105}(\mathbb{R}^2), \tilde{\phi} \in W^{0.4067}(\mathbb{R}^2)$: the non-zero impulse responses of $p(\omega)$ are

$$p_{00} = 0.98832654285769,$$
$$p_{01} = p_{10} = p_{-1-1} = 0.49156433996017,$$
$$p_{-10} = p_{0-1} = p_{11} = 0.50750780089008,$$
$$p_{-2-2} = p_{02} = p_{20} = 0.00389115238077,$$
$$p_{-3-2} = p_{-2-3} = p_{13} = p_{31} = p_{-12} = p_{2-1} = -0.00250260029669,$$
$$p_{-3-3} = p_{30} = p_{03} = p_{-2-1} = p_{-1-2} = p_{-11} = p_{1-1} = p_{21} = p_{12} = 0.00197768658105;$$

the non-zero impulse responses of $q^{(1)}(\omega)$ are

$$\begin{aligned}
&q_{00}^{(1)} = 0.03511796779580,\\
&q_{01}^{(1)} = q_{10}^{(1)} = 0.29863493249023,\\
&q_{-1-1}^{(1)} = -0.80239194082786,\\
&q_{11}^{(1)} = q_{-10}^{(1)} = q_{0-1}^{(1)} = 0.01803315183284,\\
&q_{02}^{(1)} = q_{20}^{(1)} = -0.10159057223583,\\
&q_{-2-2}^{(1)} = 0.29676935480645,\\
&q_{1-1}^{(1)} = q_{12}^{(1)} = q_{21}^{(1)} = q_{-11}^{(1)}\\
&\quad = q_{03}^{(1)} = q_{30}^{(1)} = -0.05163362721657,\\
&q_{31}^{(1)} = q_{13}^{(1)} = q_{2-1}^{(1)} = q_{-12}^{(1)} = 0.06533812386146,\\
&q_{-2-1}^{(1)} = q_{-1-2}^{(1)} = q_{-3-3}^{(1)} = 0.15083366397237,\\
&q_{-3-2}^{(1)} = q_{-2-3}^{(1)} = -0.19086764092259;
\end{aligned}$$

and $q_{\mathbf{k}}^{(2)}$, $q_{\mathbf{k}}^{(3)}$ are given by (8); the non-zero impulse responses of $\tilde{p}(\omega)$ are

$$\begin{aligned}
&\tilde{p}_{00} = 2.07524327772965,\\
&\tilde{p}_{01} = \tilde{p}_{10} = \tilde{p}_{-1-1} = 0.57048205301141,\\
&\tilde{p}_{-10} = \tilde{p}_{0-1} = \tilde{p}_{11} = 0.72714621546633,\\
&\tilde{p}_{20} = \tilde{p}_{02} = \tilde{p}_{-2-2} = -0.14011100395303,\\
&\tilde{p}_{22} = \tilde{p}_{-20} = \tilde{p}_{0-2} = -0.36957363065319,\\
&\tilde{p}_{13} = \tilde{p}_{31} = \tilde{p}_{2-1} = \tilde{p}_{-12} =\\
&\quad \tilde{p}_{-3-2} = \tilde{p}_{-2-3} = -0.14881413423887,\\
&\tilde{p}_{2-2} = \tilde{p}_{-22} = \tilde{p}_{24} = \tilde{p}_{42} =\\
&\quad \tilde{p}_{-4-2} = \tilde{p}_{-2-4} = 0.07563510434817;
\end{aligned}$$

the non-zero impulse responses of $\tilde{q}^{(1)}(\omega)$ are

$$\begin{aligned}
&\tilde{q}_{00}^{(1)} = 8.03759108770683,\ \tilde{q}_{-1-1}^{(1)} = -7.85514652959852,\\
&\tilde{q}_{01}^{(1)} = \tilde{q}_{10}^{(1)} = -4.09997773834547,\\
&\tilde{q}_{-10}^{(1)} = \tilde{q}_{0-1}^{(1)} = \tilde{q}_{11}^{(1)} = -0.03023283293225,\\
&\tilde{q}_{02}^{(1)} = \tilde{q}_{20}^{(1)} = 1.00695892898345,\\
&\tilde{q}_{-2-2}^{(1)} = 1.92923241081903,\\
&\tilde{q}_{22}^{(1)} = \tilde{q}_{-20}^{(1)} = \tilde{q}_{0-2}^{(1)} = 0.0153659024747,\\
&\tilde{q}_{31}^{(1)} = \tilde{q}_{13}^{(1)} = \tilde{q}_{2-1}^{(1)} = \tilde{q}_{-12}^{(1)} = 1.06950715506265,\\
&\tilde{q}_{2-2}^{(1)} = \tilde{q}_{-22}^{(1)} = \tilde{q}_{24}^{(1)} = \tilde{q}_{42}^{(1)} = -0.54357931582244,\\
&\tilde{q}_{-3-2}^{(1)} = \tilde{q}_{-2-3}^{(1)} = 2.04906854466516,\\
&\tilde{q}_{-2-4}^{(1)} = \tilde{q}_{-4-2}^{(1)} = -1.04144350256089;
\end{aligned}$$

and $\tilde{q}_{\mathbf{k}}^{(2)}$, $\tilde{q}_{\mathbf{k}}^{(3)}$ are given by (8).

Appendix D

The biorthogonal filters in Example 6 with $\phi \in W^{1.5105}(\mathbb{R}^2), \tilde{\phi} \in W^{0.4067}(\mathbb{R}^2)$: the non-zero impulse response coefficients of $p(\omega)$ are

$$\begin{aligned}
&p_{00} = 0.98832654285769,\\
&p_{01} = p_{10} = p_{-1-1} = 0.49156433996017,\\
&p_{-10} = p_{0-1} = p_{11} = 0.50750780089008,\\
&p_{-2-2} = p_{02} = p_{20} = 0.00389115238077,\\
&p_{-3-2} = p_{-2-3} = p_{13} = p_{31} =\\
&\quad p_{-12} = p_{2-1} = -0.00250260029669,\\
&p_{-3-3} = p_{30} = p_{03} = p_{-2-1} = p_{-1-2} = p_{-11} = p_{1-1}\\
&= p_{21} = p_{12} = 0.00197768658105;
\end{aligned}$$

the non-zero impulse response coefficients of $q^{(1)}(\omega)$ are

$$\begin{aligned}
&q_{00}^{(1)} = 0.03511796779580,\\
&q_{01}^{(1)} = q_{10}^{(1)} = 0.29863493249023,\\
&q_{-1-1}^{(1)} = -0.80239194082786,\\
&q_{11}^{(1)} = q_{-10}^{(1)} = q_{0-1}^{(1)} = 0.01803315183284,\\
&q_{02}^{(1)} = q_{20}^{(1)} = -0.10159057223583,\\
&q_{-2-2}^{(1)} = 0.29676935480645,\\
&q_{1-1}^{(1)} = q_{12}^{(1)} = q_{21}^{(1)} = q_{-11}^{(1)}\\
&\quad = q_{03}^{(1)} = q_{30}^{(1)} = -0.05163362721657,\\
&q_{31}^{(1)} = q_{13}^{(1)} = q_{2-1}^{(1)} = q_{-12}^{(1)} = 0.06533812386146,\\
&q_{-2-1}^{(1)} = q_{-1-2}^{(1)} = q_{-3-3}^{(1)} = 0.15083366397237,\\
&q_{-3-2}^{(1)} = q_{-2-3}^{(1)} = -0.19086764092259,
\end{aligned}$$

and $q_{\mathbf{k}}^{(2)}$, $q_{\mathbf{k}}^{(3)}$ are given by (8); the non-zero impulse response coefficients of $\tilde{p}(\omega)$ are

$$\begin{aligned}
&\tilde{p}_{00} = 2.07524327772965,\\
&\tilde{p}_{01} = \tilde{p}_{10} = \tilde{p}_{-1-1} = 0.57048205301141,\\
&\tilde{p}_{-10} = \tilde{p}_{0-1} = \tilde{p}_{11} = 0.72714621546633,\\
&\tilde{p}_{20} = \tilde{p}_{02} = \tilde{p}_{-2-2} = -0.14011100395303,\\
&\tilde{p}_{22} = \tilde{p}_{-20} = \tilde{p}_{0-2} = -0.36957363065319,\\
&\tilde{p}_{13} = \tilde{p}_{31} = \tilde{p}_{2-1} = \tilde{p}_{-12} =\\
&\quad \tilde{p}_{-3-2} = \tilde{p}_{-2-3} = -0.14881413423887,\\
&\tilde{p}_{2-2} = \tilde{p}_{-22} = \tilde{p}_{24} = \tilde{p}_{42} =\\
&\quad \tilde{p}_{-4-2} = \tilde{p}_{-2-4} = 0.07563510434817;
\end{aligned}$$

the non-zero impulse response coefficients of $\tilde{q}^{(1)}(\omega)$ are

$$\begin{aligned}
&\tilde{q}_{00}^{(1)} = 8.03759108770683,\ \tilde{q}_{-1-1}^{(1)} = -7.85514652959852,\\
&\tilde{q}_{01}^{(1)} = \tilde{q}_{10}^{(1)} = -4.09997773834547,\\
&\tilde{q}_{-10}^{(1)} = \tilde{q}_{0-1}^{(1)} = \tilde{q}_{11}^{(1)} = -0.03023283293225,\\
&\tilde{q}_{02}^{(1)} = \tilde{q}_{20}^{(1)} = 1.00695892898345,\\
&\tilde{q}_{-2-2}^{(1)} = 1.92923241081903,\\
&\tilde{q}_{22}^{(1)} = \tilde{q}_{-20}^{(1)} = \tilde{q}_{0-2}^{(1)} = 0.0153659024747,\\
&\tilde{q}_{31}^{(1)} = \tilde{q}_{13}^{(1)} = \tilde{q}_{2-1}^{(1)} = \tilde{q}_{-12}^{(1)} = 1.06950715506265,\\
&\tilde{q}_{2-2}^{(1)} = \tilde{q}_{-22}^{(1)} = \tilde{q}_{24}^{(1)} = \tilde{q}_{42}^{(1)} = -0.54357931582244,\\
&\tilde{q}_{-3-2}^{(1)} = \tilde{q}_{-2-3}^{(1)} = 2.04906854466516,\\
&\tilde{q}_{-2-4}^{(1)} = \tilde{q}_{-4-2}^{(1)} = -1.04144350256089,
\end{aligned}$$

and $\tilde{q}^{(2)}_{\mathbf{k}} = \tilde{q}^{(1)}_{R_1\mathbf{k}}$, $\tilde{q}^{(3)}_{\mathbf{k}} = \tilde{q}^{(1)}_{R_2\mathbf{k}}$.

Some publications, some more

ACKNOWLEDGMENT

The author thanks James D. Allen and Xiqiang Zheng for providing preprints [4] and [9]. The author is very grateful to the anonymous reviewers for making many valuable suggestions that significantly improve the presentation of the paper.

REFERENCES

[1] D.P. Petersen and D. Middleton, "Sampling and reconstruction of wave-number-limited functions in N-dimensional Euclidean spaces", *Information and Control*, vol. 5, no. 4, pp. 279-323, Dec. 1962.

[2] R.M. Mersereau, "The processing of hexagonal sampled two-dimensional signals", *Proc. IEEE*, vol. 67, no. 6, pp. 930–949, Jun. 1979.

[3] R.C. Staunton and N. Storey, "A comparison between square and hexagonal sampling methods for pipeline image processing", In *Proc. of SPIE Vol. 1194, Optics, Illumination, and Image Sensing for Machine Vision IV*, 1990, pp. 142–151.

[4] J.D. Allen, "Coding transforms for the hexagon grid", Ricoh Calif. Research Ctr., Technical Report CRC-TR-9851, Aug. 1998.

[5] G. Tirunelveli, R. Gordon, and S. Pistorius, "Comparison of square-pixel and hexagonal-pixel resolution in image processing", in *Proceedings of the 2002 IEEE Canadian Conference on Electrical and Computer Engineering*, vol. 2, May 2002, pp. 867–872.

[6] D. Van De Ville, T. Blu, M. Unser, W. Philips, I. Lemahieu, and R. Van de Walle, "Hex-splines: a novel spline family for hexagonal lattices", *IEEE Tran. Image Proc.*, vol. 13, no. 6, pp. 758–772, Jun. 2004.

[7] L. Middleton and J. Sivaswarmy, *Hexagonal Image Processing: A Practical Approach*, Springer, 2005.

[8] X.J. He and W.J. Jia, "Hexagonal Structure for Intelligent Vision", in *Proceedings of the 2005 First International Conference on Information and Communication Technologies*, Aug. 2005, pp. 52–64.

[9] X.Q. Zheng, G.X. Ritter, D.C. Wilson, and A. Vince, "Fast discrete Fourier transform algorithms on regular hexagonal structures", preprint, University of Florida, Gainsville, FL, 2006.

[10] R.C. Staunton, "The design of hexagonal sampling structures for image digitization and their use with local operators", *Image and Vision Computing*, vol. 7, no. 3, pp. 162–166, Aug. 1989.

[11] L. Middleton and J. Sivaswarmy, "Edge detection in a hexagonal-image processing framework", *Image and Vision Computing*, vol. 19, no. 14, pp. 1071-1081, Dec. 2001.

[12] A.F. Laine, S. Schuler, J. Fan, and W. Huda, "Mammographic feature enhancement by multiscale analysis", *IEEE Trans. Med Imaging*, vol. 13, no. 4, pp. 725–740, Dec. 1994.

[13] A.F. Laine and S. Schuler, "Hexagonal wavelet representations for recognizing complex annotations", in *Proceedings of the IEEE Conference on Computer Vision and Pattern Recognition*, Seattle, WA, Jun. 1994, pp. 740-745.

[14] A.P. Fitz and R. Green, "Fingerprint classification using hexagonal fast Fourier transform", *Pattern Recognition*, vol. 29, no. 10, pp. 1587–1597, 1996.

[15] S. Periaswamy, "Detection of microcalcification in mammograms using hexagonal wavelets", M.S. thesis, Dept. of Computer Science, Univ. of South Carolina, Columbia, SC, 1996.

[16] R.C. Staunton, "One-pass parallel hexagonal thinning algorithm", *IEE Proceedings on Vision, Image and Signal Processing*, vol. 148, no. 1, pp. 45–53, Feb. 2001.

[17] A. Camps, J. Bara, I.C. Sanahuja, and F. Torres, "The processing of hexagonally sampled signals with standard rectangular techniques: application to 2-D large aperture synthesis interferometric radiometers", *IEEE Trans. Geoscience and Remote Sensing*, vol. 35, no. 1, pp. 183–190, Jan. 1997.

[18] E. Anterrieu, P. Waldteufel, and A. Lannes, "Apodization functions for 2-D hexagonally sampled synthetic aperture imaging radiometers", *IEEE Trans. Geoscience and Remote Sensing*, vol. 40, no. 12, pp. 2531–2542, Dec. 2002.

[19] D. White, A.J. Kimberling, and W.S. Overton, "Cartographic and geometric components of a global sampling design for environmental monitoring", *Cartography and Geographic Information Systems*, vol. 19, no. 1, pp. 5-22, 1992.

[20] K. Sahr, D. White, and A.J. Kimerling, "Geodesic discrete global grid systems", *Cartography and Geographic Information Science*, vol. 30, no. 2, pp. 121–134, Apr. 2003.

[21] E.A. Adelson, E. Simoncelli, and R. Hingorani, "Orthogonal pyramid transforms for image coding", In *SPIE Visual Communications and Image Processing II* (1987), vol. 845, 1987, pp. 50–58.

[22] A.B. Watson and A. Ahumada, Jr., "A hexagonal orthogonal-oriented pyramid as a model of image presentation in visual cortex", *IEEE Trans. Biomed. Eng.*, vol. 36, no. 1, pp. 97–106, Jan. 1989.

[23] E. Simoncelli and E. Adelson, "Non-separable extensions of quadrature mirror filters to multiple dimensions", *Proceedings of the IEEE*, vol. 78, no. 4, pp. 652–664, Apr. 1990.

[24] H. Xu, W.-S. Lu, and A. Antoniou, "A new design of 2-D non-separable hexagonal quadrature-mirror-filter banks", in *Proc. CCECE*, Vancouver, Sep. 1993, pp. 35–38.

[25] A. Cohen and J.-M. Schlenker, "Compactly supported bidimensional wavelets bases with hexagonal symmetry", *Constr. Approx.*, vol. 9, no. 2/3, pp. 209–236, Jun. 1993.

[26] J.D. Allen, "Perfect reconstruction filter banks for the hexagonal grid", In *Fifth International Conference on Information, Communications and Signal Processing 2005*, Dec. 2005, pp. 73–76.

[27] C. Cabrelli, C. Heil, and U. Molter, "Accuracy of lattice translates of several multidimensional refinable functions", *J. Approx. Theory*, vol. 95, no. 1, pp. 5–52, Oct. 1998.

[28] R.Q. Jia, "Convergence of vector subdivision schemes and construction of biorthogonal multiple wavelets", In *Advances in Wavelets*, Springer-Verlag, Singapore, 1999, pp. 199–227.

[29] W. Lawton, S.L. Lee, and Z.W. Shen, "Stability and orthonormality of multivariate refinable functions", *SIAM J. Math. Anal.*, vol. 28, no. 4, pp. 999–1014, Jul. 1997.

[30] C.K. Chui and Q.T. Jiang, "Multivariate balanced vector-valued refinable functions", in *Mordern Development in Multivariate Approximation*, ISNM 145, Birhhäuser Verlag, Basel, 2003, pp. 71–102.

[31] M. Vetterli and J. Kovacevic, *Wavelets and Subband Coding*, Prentice Hall, 1995.

[32] G. Strang and T. Nguyen, *Wavelets and Filter Banks*, Wellesley-Cambridge Press, 1996.

[33] R.Q. Jia, "Approximation properties of multivariate wavelets", *Math. Comp.*, vol. 67, no. 222, pp. 647–665, Apr. 1998.

[34] Q.T. Jiang, "Orthogonal multiwavelets with optimum time–frequency resolution", *IEEE Trans. Signal Proc.*, vol. 46, no. 4, pp. 830–844, Apr. 1998.

[35] Q.T. Jiang, "On the design of multifilter banks and orthonormal multiwavelet bases", *IEEE Trans. Signal Proc.*, vol. 46, no. 12, pp. 3292–3303, Dec. 1998.

[36] R.Q. Jia and S.R. Zhang, "Spectral properties of the transition operator associated to a multivariate refinement equation", *Linear Algebra Appl.*, vol. 292, no. 1, pp. 155–178, May 1999.

[37] R.Q. Jia and Q.T. Jiang, "Spectral analysis of transition operators and its applications to smoothness analysis of wavelets", *SIAM J. Matrix Anal. Appl.*, vol. 24, no. 4, pp. 1071–1109, 2003.

[38] Q.T. Jiang and P. Oswald, "Triangular $\sqrt{3}$-subdivision schemes: the regular case", *J. Comput. Appl. Math.*, vol. 156, no. 1, pp. 47–75, Jul. 2003.

PLACE PHOTO HERE

Qingtang Jiang received his B.S. and M.S. degrees from Hangzhou University, Hangzhou, China, in 1986 and 1989, respectively, and his Ph.D. degree from Peking University, Beijing, China, in 1992, all in mathematics. He was with Peking University, Beijing, China from 1992 to 1995. He was an NSTB post-doctoral fellow and research fellow at the National University of Singapore from 1995 to 1997. Before joined University of Missouri - St. Louis in 2002, he held visting positions at Unversity of Alberta, Canada, and West Virginia University, USA. He is now a full professor in the Department of Math and Computer Science at University of Missouri - St. Louis. Dr. Jiang's current research interests include time–frequency analysis, wavelet theory and its applications, filter bank design, signal classification, image processing and surface subdivision.